2.4. Immunohistochemistry

Cytoplasmic tryptase was examined by immunohistochemistry using a DAKO envision kit. In brief, cytospin preparations were fixed with 4% PFA in PBS. After washing, endogenous peroxidase was inactivated with 0.3% H_2O_2 in methanol. After washing, samples were blocked with 2% goat serum in PBS for 30 min at RT, and then stained with mouse anti-tryptase antibody (AA1; Serotec, Oxford, UK) for 30 min at RT. Mouse IgG1 (BD Bioscience, San Jose, CA) was used as an isotype control. As secondary antibody, horseradish peroxidase (HRP)-conjugated goat anti-mouse IgG antibody included in the kit was applied for 30 min at RT, and 3,3′-diaminobenzidine tetrahydrochloride (DAB) was used as a substrate. Nuclei were stained with haematoxylin.

2.5. Flow cytometric analysis

To detect cell surface KIT expression, the cells were incubated with 1% rat serum in PBS for 30 min at 4 °C, and then stained with phycoerythrin (PE)-labeled rat anti-mouse c-kit antibody (2B8; BD Biosciences) for 30 min at 4 °C. Isotype-matched PE-labeled rat IgG2b (BD Biosciences) was used as a negative control. To examine FcεRI expression on cell surface, cells were incubated with 1% goat serum in PBS for 30 min at 4 °C, and then incubated with monoclonal dog IgE (5 μg/ml; Bethyl Laboratories, Montgomery, TX) for 30 min at 4 °C. After washing, cell surface IgE bound to FcεRI was detected with fluorescein isothiocyanate (FITC)-labeled goat anti-dog IgE antibody (Bethyl Laboratories) by incubation for 30 min at 4 °C. Isotype-matched FITC-labeled goat IgG antibody (Jackson ImmunoResearch Laboratories, West Grove, PA) was used as a negative control. Expression of KIT and FcεRI was analyzed by flow cytometory (FACSCalibur; BD Biosciences) with CellQuest software (BD Biosciences).

2.6. Histamine contents

Cells were lysed with CelLytic-M buffer (Sigma–Aldrich), and histamine contents in the cell lysate were measured by a commercially available ELISA kit (IBL Immuno Biological Laboratories, Hamburg, Germany).

2.7. β-Hexosaminidase release assay

To assess FcεRI-mediated degranulation, 1×10^6 cells were passively sensitized with 20% IgE-rich dog serum in Tyrode's buffer (130 mM NaCl, 5 mM KCl, 1.4 mM $CaCl_2$, 1 mM $MgCl_2$, 5.6 mM glucose, 10 mM HEPES and 0.1% BSA, pH 7.4) for 1 h at 4 °C and then stimulated with various concentrations of anti-dog IgE antibody (Bethyl Laboratories) in 100 μl of Tyrode's buffer for 1 h at 37 °C. To measure FcεRI-independent degranulation, 1×10^6 cells were stimulated with various concentrations of calcium ionophore A23187 (Sigma–Aldrich) in 100 μl of Tyrode's buffer for 1 h at 37 °C. Cytotoxicity of each stimulus was examined by a trypan blue dye exclusion test. After stimulation, the supernatant was collected and the cells were lysed in Tyrode's buffer containing 0.5% triton X. β-Hexosaminidase activity in the supernatant and the cell lysate was measured by hydrolysis of *p*-nitrophenyl-*N*-acetyl-β-D-glucopyranoside (Sigma–Aldrich) in 0.1 M sodium citrate buffer (pH 4.5) for 40 min at 37 °C. The percentage of β-hexosaminidase release was calculated as follows: (β-hexosaminidase release by each stimulus − spontaneous β-hexosaminidase release)/(total β-hexosaminidase activity − spontaneous β-hexosaminidase release) × 100.

2.8. RT-PCR

Total RNA extracted from HRMC cells was used for cDNA synthesis as described previously (Ohmori et al., 2004). Using the primers listed in Table 1, FcεRIα, β, FcRγ, CD23, β-actin and four fragments of an open reading frame of *c-kit* were amplified by RT-PCR with a TAKARA Ex Taq (TAKARA, Shiga, Japan). A canine lymphoma cell line (CL-1) (Momoi et al., 1997) was used as a negative control. The PCR amplification consisted of pre-denaturation (94 °C, 2 min), and 35 cycles of denaturation (94 °C, 2 min), annealing (55 °C for FcεRIα, β, FcRγ, CD23, and β-actin, 60 °C for *c-kit*, 1 min), and extension (72 °C, 1 min; *c-kit* fragment 1: 72 °C, 3 min), followed by final extension (72 °C, 8 min).

2.9. Nucleotide sequence of an open reading frame of c-kit cDNA and genomic DNA of the juxtamembrane domain of c-kit

Four fragments of an open reading frame of *c-kit* were amplified by RT-PCR. To amplify the juxtamembrane domain (exon 11, intron 11, and exon 12) of *c-kit*, genomic DNA was extracted from HRMC cells with a Wizard Genomic DNA Purification kit (Promega, Madison, WI). Genomic PCR was performed with the same PCR condition described above

Table 1
Nucleotide sequence of RT-PCR and sequence primers

Gene	Primer	Sequence (5′-3′)
FcεRIα chain	Forward	GCGCTGCTGCTCTCCTCTCC
	Reverse	TAGTTGCCGCTGTTTTTGGTTGTG
FcεRIβ chain	Forward	TTCTGGGGGTAACACAAAT
	Reverse	TGCAAAACCCCAGAATAGT
FcRγ chain	Forward	ATTTCTGCCGTGGTCTTGCTCCTG
	Reverse	GTCTCCTGGTTCCGGGTGCTCA
CD23	Forward	CCCAGAGCTTGAACGAGAGAA
	Reverse	TCCTCGCCGAAGTAGTAGCAC
β-Actin	Forward	TGTGGCCATCCAGGCTGTGC
	Reverse	GTGGTCTCGTGGATACCGCA
c-kit cDNA fragment 1	Forward	AGTCTATCGCAGCCACCGC
	Reverse	GAAGGCACCAGCACCCAAAGT
c-kit cDNA fragment 2	Forward	GAGGAGATCAATGGAAACAATTATG
	Reverse	GTGAATACAATTCTTGGAGGCGAGG
c-kit cDNA fragment 3	Forward	CACCCTGGTCATTACAGAATATTG
	Reverse	CGGAAGCCTTCCTTGATCATCTTG
c-kit cDNA fragment 4	Forward	AAAGGAAACGCTCGGCTACCTG
	Reverse	GGACAGAATAACCAGTATAGGAAC
c-kit genomic DNA juxtamembrane domain	Forward	CAAATCCATCCCCACACCCTGTTCA
	Reverse	AGCATCTTAACGGCAACAGTCA
Sequence primer (*c-kit* cDNA frgament 1)		GCAATTACACGTGCACCAAC
		TACATTGTTGTAAGCCCTAC
		AAGCTCTCTCCTGAAGGAAG

(extension time: 1 min) using the primer pair in Table 1. PCR products of *c-kit* cDNA and genomic DNA were subcloned into a pGEM-T Easy Vector (Promega, Madison, WI) and sequenced as described previously (Ohmori et al., 2004). For sequencing the fragment 1 of *c-kit* cDNA, three internal primes in Table 1 were used. More than 10 independent clones of the each plasmid were sequenced.

2.10. Cell proliferation assay

Cells (2×10^5 cells/ml) were cultured in AIM-V in a 96-well plate with various concentrations of STI571 (kindly provided by Novartis, Basel, Switzerland) for the indicated time periods. The cell viability in the wells were measured by using a Cell CountingKit-8 (Dojindo, Kumamoto, Japan) with WST-8 [2-(2-methoxy-4-nitrophenyl)-3-(4-nitrophenyl)-5-(2,4-disulfophenyl)-2H-tetrazolium, monosodium salt] as a substrate. Absorbance was measured at 450 nm with a microplate reader (Model 550; Bio-Rad Laboratories, Hercules, CA).

3. Results

3.1. Clinical outcome of a dog with MCT

MCT in the right forelimb of a 12-year-old male Golden retriever (histological grade II: intermediately differentiated MCT according to the grading criteria; Patnaik et al., 1984) was removed by an surgical operation. Since metastasis of MCT to the superficial cervical lymph node was found 2 months after the operation, a whole right forelimb and the lymph node were resected. Vinblastine was administered to the dog once a week with daily methylprednisolone for 4 weeks, and additional vinblastine treatment was performed once every 2 weeks with daily methylprednisolone for further 6 weeks. However, MCT recurred on the thoracic skin of the dog, and eventually, the dog resulted in death.

3.2. Cell growth

MCT cells isolated from the dog at the first surgical operation were cultured in serum-free AIM-V medium

that was shown to be useful for the culture of skin-derived normal human mast cells (Kambe et al., 2001). The cells showed apparent and continuous cell growth 3 months after the initiation of the cell culture. A cell line with continuous proliferation could be established after approximately 30 passages and named as HRMC. The log phase doubling time of the cell growth was 56.8 ± 4.2 h.

3.3. Ultrastructural, cytochemical and immunohistochemical analysis

A transmission electron microscopic analysis revealed that HRMC cells had relatively round cytoplasm with irregular shape of cell membrane and few cytoplasmic projections (Fig. 1(A)). HRMC cells had an oval to round nucleus with a prominent nucleolus. Few granules were observed in the cytoplasm, and these were heterogeneous in their size, shape and electron density (Fig. 1(B)). Ultrastructural appearance of HRMC cells was similar to that of the immature canine neoplastic mast cells shown in the previous reports (Garcia et al., 1998; Ishiguro et al., 2001; Takahashi et al., 2001).

HRMC cells had cytoplasmic metachromatic granules as indicated by toluidine blue staining of the cytospin samples (Fig. 1(C)). However, the number of metachromatic granules in HRMC cells was smaller than that in normal canine mast cells (Lin et al., 2006). Cytochemical staining for chymase showed positive cytoplasmic granules (Fig. 1(D)). Immunohistochemical analysis demonstrated the presence of cytoplasmic tryptase in HRMC cells (Fig. 1(E)).

3.4. Expression of KIT and FcεRI on HRMC cells

Mast cells are characterized by co-expression of KIT and the high-affinity IgE receptor, FcεRI, on the cell surface (Galli et al., 2005; Gilfillan and Tkaczyk, 2006). Flow cytometric analysis revealed that HRMC cells expressed KIT on the cell surface (Fig. 2(A)). We could also detect cell surface IgE that bound to IgE receptors on HRMC cells (Fig. 2(B)). IgE was shown to bind to FcεRI and the low-affinity IgE receptor (CD23) (Gould et al., 2003). We, therefore, analyzed mRNA expression of FcεRI and CD23 in HRMC cells. As shown in Fig. 2(C), HRMC cells, but not a canine lymphoma cell line, CL1, expressed mRNA of FcεRI components, FcεRIα, β and FcRγ chains, although they showed slight expression of CD23 mRNA. Thus, we concluded that HRMC cells expressed both KIT and FcεRI on the cell surface.

3.5. Histamine contents and β-hexosaminidase release

We next examined histamine contents and degranulation in HRMC cells. HRMC cells were found to contain 0.032 ± 0.007 pg of histamine per cell. To assess the degranulation of HRMC cells, we carried out β-hexosaminidase release assay. HRMC cells released 6.7% of β-hexosaminidase through FcεRI cross-linking at a maximum (Fig. 3(A)). As shown in other canine MCT cell lines (Brazis et al., 2002; Garcia et al., 1998), the percentage of β-hexosaminidase release by FcεRI cross-linking in HRMC cells was lower than that in bone marrow-derived cultured canine mast cells (Lin et al., 2006). However, stimulation of HRMC cells with calcium ionophore A23187 induced up to 18.6% of β-hexosaminidase release in a dose-dependent manner (Fig. 3(B)).

3.6. Nucleotide sequence analysis of c-kit

To investigate an involvement of *c-kit* mutations in the neoplastic proliferation of HRMC cells, we determined the nucleotide sequence of an open reading frame of *c-kit* cDNA in HRMC cells. Compared with the sequence of normal dog *c-kit* (GenBank accession no. AY313776), *c-kit* in HRMC cells was found to have two different nucleotide substitutions at codon 159 (C → T) and codon 507 (A → G); however, these nucleotide substitutions were reported as single nucleotide polymorphisms (SNPs) in normal dog *c-kit* (GenBank accession no. AF448148) (Tsai et al., 2003). The SNPs found in *c-kit* of HRMC cells did not lead to amino acid substitutions. Accordingly, the deduced amino acid sequence of *c-kit* in HRMC cells was shown to have 100% homology with that of normal dog *c-kit* (GenBank accession no. AY313776) and did not contain any mutations such as duplications, deletions and substitutions as shown in canine MCTs in the previous reports (London et al., 1999; Ma et al., 1999).

In the process of the sequence analysis, we found two isoforms of *c-kit* at the junction of exon 4 and exon 5 (Fig. 4(A)). These two isoforms were reported as normal dog *c-kit* sequences (GenBank accession nos. AF044249 and AF099030). We also confirmed expression of these two isoforms of *c-kit* in the thymus of a normal dog (data not shown). The 3-bp deleted isoform was less frequently observed in *c-kit* of HRMC cells and a normal dog. Thus, the 3-bp deleted isoform identified between exon 4 and exon 5 was considered an alternative splicing variant. In normal dog *c-kit*, another

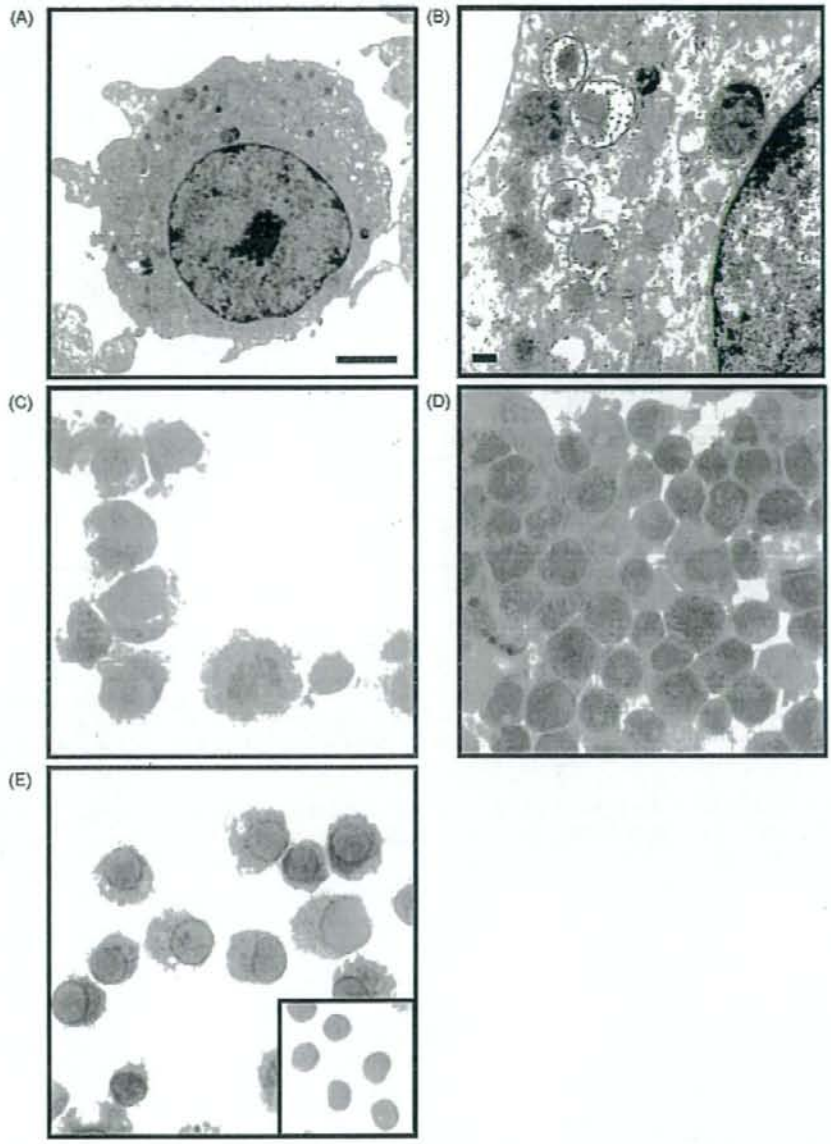

Fig. 1. Ultrastructural, cytochemical and immunohistochemical analysis of HRMC cells. (A) Ultrastructural appearance of the nucleus and the cytoplasm. Bar indicates 2 μm. (B) Ultrastructure of intracytoplasmic granules. Bar indicates 0.2 μm. Ultrastructures of HRMC cells were analyzed by a transmission electronic microscope. (C) Toluidine blue staining of HRMC cells. (D) Cytoplasmic chymase of HRMC cells. Chymase was detected with naphthol-AS-D-chloroacetate as a substrate and Fast Red Violet LB salt as dye. (E) Cytoplasmic tryptase of HRMC cells. Tryptase was analyzed by immunohistochemistry with an isotype control (insert). The data are representative of more than three independent experiments.

alternative splicing variant that has additional 12-bp to the normal sequence has been demonstrated at the junction of exon 9 and exon 10 (London et al., 1999; Tsai et al., 2003). This alternative splicing variant was also found in *c-kit* of HRMC cells together with the dominant normal *c-kit* sequence (Fig. 4(B)).

We further examined the nucleotide sequence of genomic DNA at the juxtamembrane domain of *c-kit* in

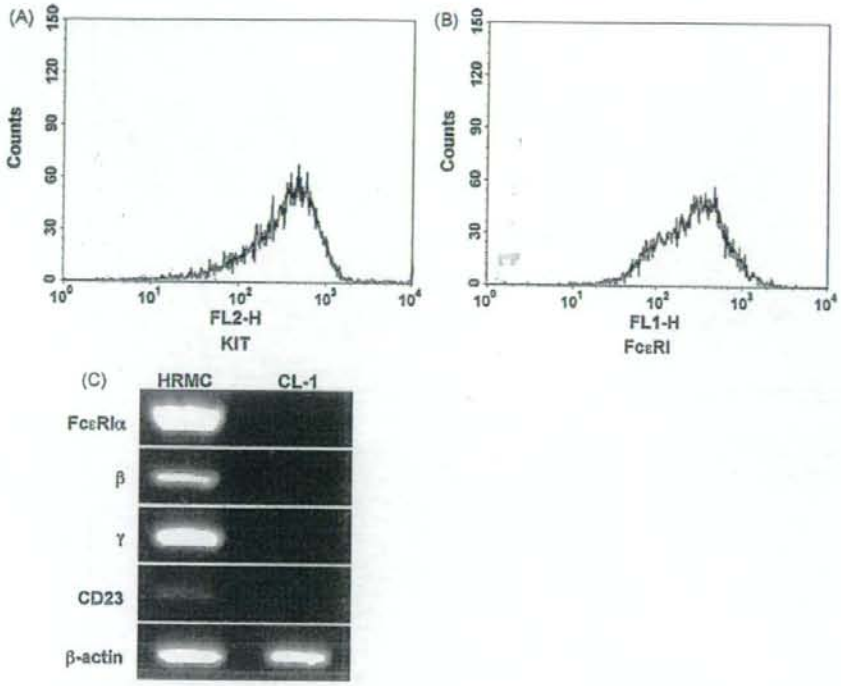

Fig. 2. Expression of KIT and FcεRI on HRMC cells. (A) KIT on HRMC cells were stained with PE-labeled rat anti-mouse c-kit antibody (black line). (B) To detect FcεRI expression, HRMC cells were incubated with monoclonal dog IgE, and then stained with FITC-labeled goat anti-dog IgE antibody (black line). PE or FITC-labeled isotype matched antibodies were used as negative controls (gray shade). (C) mRNA expression of FcεRIα, β, FcR-γ and CD23 in HRMC cells was detected by RT-PCR. β-Actin was used as an internal control. The data are representative of 2–3 independent experiments.

HRMC cells. We amplified and sequenced genomic *c-kit* DNA from exon 10 to exon 12 in HRMC cells, and compared the sequence with that in normal dog cells. As shown in Fig. 5, *c-kit* mutations previously identified in canine MCTs such as duplications, deletions, or point mutations were not found in the juxtamembrane domain of *c-kit* in HRMC cells. Nucleotide substitutions at three different positions were detected in intron 11 of *c-kit* in

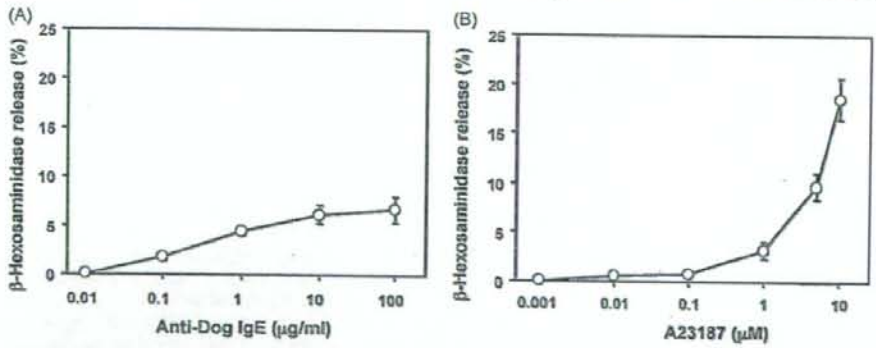

Fig. 3. β-Hexosaminidase release from HRMC cells by FcεRI cross-linking or calcium ionophore A23187 stimulation. (A) For FcεRI cross-linking, cells were incubated with a 20% IgE-rich dog serum to saturate FcεRI with dog IgE, and then stimulated with increasing concentrations of anti-dog IgE antibody. (B) As FcεRI-independent stimulation, cells were incubated with increasing concentrations of calcium ionophore A23187. Cytotoxicity of each stimulus was examined by a trypan blue exclusion test. Percentage of β-hexosaminidase release from HRMC cells were calculated as described in materials and methods. The data represent the mean ± S.D. of five independent experiments.

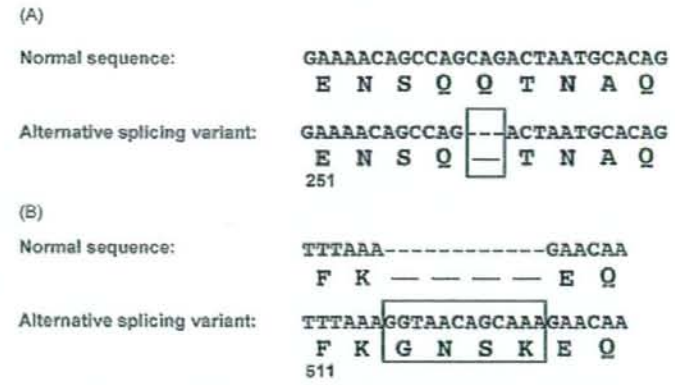

Fig. 4. Nucleotide sequence of alternative splicing variants of *c-kit* identified in HRMC cells. (A) An alternative splicing variant at the junction of exons 4 and 5. (B) An alternative splicing variant at the junction of exons 9 and 10.

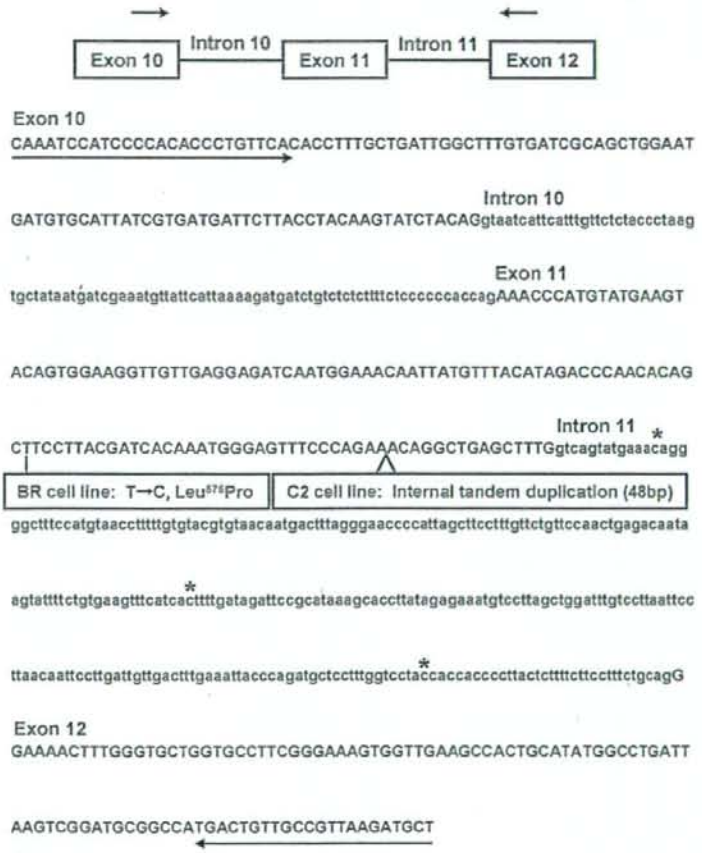

Fig. 5. Nucleotide sequence of genomic DNA in the juxtamembrane domain of *c-kit* in HRMC cells. Upper and lower case letters represent exon and intron, respectively. Asterisks indicate SNPs. Arrows mean primers.

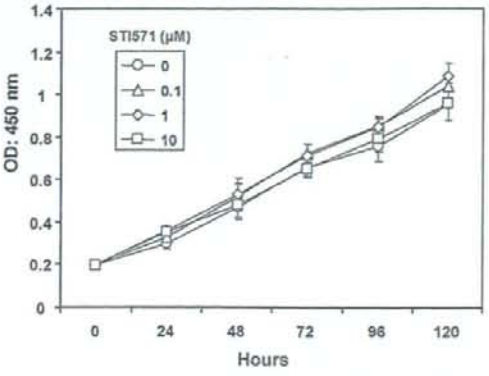

Fig. 6. Effect of STI571 on proliferation of HRMC cells. HRMC cells were cultured in the presence of indicated concentrations of STI571 for 120 h. Viability of cells was determined by WST-8 assay. The data represent mean ± S.D. of three independent experiments.

HRMC cells as SNPs (Fig. 5), consistent with the previous study which reported SNPs at the same positions (Zemke et al., 2002).

3.7. Effect of STI571 on the proliferation of HRMC cells

STI571, imatinib mesylate, is a receptor tyrosine kinase inhibitor (Akin and Metcalfe, 2004) and was shown to have an inhibitory effect on cell proliferation of human and mouse mast cell tumors carrying activating mutations in the juxtamembrane domain of *c-kit* (Ma et al., 2002; Zermati et al., 2003). To evaluate an inhibitory effect of STI571 on the proliferation of HRMC cells, the cells were cultured in serum-free AIM-V with increasing concentrations of STI571 for 24, 48, 72, 96 and 120 h. The cell viability of HRMC cells was assessed at each time point. As shown in Fig. 6, HRMC cells were capable of proliferating in the presence of STI571 at comparable levels in the absence of STI571, indicating that STI571 did not have any inhibitory effects on the proliferation of HRMC cells at concentrations up to 10 μM.

4. Discussion

In the present study, we established a growth factor-independent mast cell tumor cell line, HRMC, from a dog with MCT. The characterization of HRMC cells revealed cytoplasmic metachromatic granules, chymase, and tryptase, and expression of FcεRI and KIT on the cell surface. HRMC cells contained histamine and released β-hexosaminidase through FcεRI cross-linking and calcium ionophore stimulation. These results indicate that HRMC cells possess the phenotypes characteristic of mast cells.

Sequence analysis of *c-kit* gene did not find any mutations in HRMC cells. Recent studies have shown the heterogeneity of cancer cells and provided the concept of cancer stem cells (Dalerba et al., 2007). Thus, there might be a possibility that original MCT which HRMC cells derived from was composed of *c-kit* mutation-positive and -negative cells, and only the mutation-negative HRMC stem cells might have proliferated during culture process. However, the important finding obtained in this study is that HRMC cells could grow without *c-kit* gene mutations, as supported by the observation that STI571 did not have any inhibitory effects on the proliferation of HRMC cells at concentrations up to 10 μM. Although mutations in the juxtamembrane domain of *c-kit* have been considered the pivotal molecular mechanism capable of initiating neoplastic transformation of mast cells in dogs (London et al., 1999; Ma et al., 1999), the present study clearly demonstrates that *c-kit* mutations-independent mechanism(s) can also regulate neoplastic proliferation of mast cells in dogs.

The receptor tyrosine kinase inhibitors were shown to suppress the proliferation of canine mast cell lines and spontaneous canine MCTs associated with mutations in the juxtamembrane domain of *c-kit* (Liao et al., 2002; Pryer et al., 2003). These results indicate that KIT can be a molecular target of therapeutic intervention in canine MCTs carrying activating mutations in the juxtamembrane domain of *c-kit*. In the present study, it was demonstrated that a tyrosine kinase inhibitor, STI571, did not inhibit the cell proliferation of HRMC cells, suggesting that KIT would not be a therapeutic target in *c-kit* mutations-independent naoplastic mast cell growth. Canine MCTs with aggressive behavior require novel molecular targeted therapies. Therefore, it is pivotal to reveal *c-kit* mutations-independent molecular mechanism(s) of canine MCTs and identify molecular target(s) of this disease.

In the previous studies that analyzed correlation of mutations in the juxtamembrane domain of *c-kit* with histological grade of MCTs in dogs, mutations were more frequently found in immature and aggressive types of MCT than mature and benign types of MCT (Downing et al., 2002; Zemke et al., 2002). This suggested that mutations in the juxtamembrane domain of *c-kit* were associated with not only initiation but also aggressive and malignant progression of MCTs in dogs. In the present study, however, we found that *c-kit* mutations-negative MCT could proliferate and behave

in a malignant manner. Since there have been no reports which investigated whole sequence of *c-kit* and analyzed a relationship between *c-kit* mutations and prognosis in canine MCTs, we can not conclude whether *c-kit* mutations are implicated in the high incidence and clinical heterogeneity of MCTs in dogs. In addition to the current pathological grading of canine MCTs proposed by Patnaik et al. (1984), it is necessary to establish the molecular classification of canine MCTs based on the *c-kit* mutations. Furthermore, it is also crucial to examine an association between the molecular classification and clinical outcomes including reactions to therapies in dogs with MCTs. These studies would be able to improve our understandings of canine MCTs and provide clinically useful findings regarding the treatment of canine MCTs.

Taken together, we demonstrated the presence of neoplastic cell growth of mast cells in the absence of mutations in *c-kit*. Further investigation of *c-kit* mutations-independent mechanisms of aberrant mast cell proliferation is essential for elucidating the pathogenesis and clinical heterogeneity of MCTs in dogs. Thus, growth factor-independent HRMC cells established in this study are considered a useful cell line to explore the mechanisms of *c-kit* mutations-independent neoplastic growth of mast cells.

Acknowledgements

We would like to thank Novartis Pharma AG for supplying STI571. This work was supported by a Grant-in-Aid for Scientific Research from the Ministry of Education, Culture, Sports, Science and Technology, Japan.

References

Akin, C., Metcalfe, D.D., 2004. The biology of Kit in disease and the application of pharmacogenetics. The Journal of Allergy and Clinical Immunology 114, 13–19 quiz 20.

Brazis, P., Torres, R., Queralt, M., de Mora, F., Ferrer, L., Puigdemont, A., 2002. Evaluation of cell-surface IgE receptors on the canine mastocytoma cell line C2 maintained in continuous culture. American Journal of Veterinary Research 63, 763–766.

Dalerba, P., Cho, R.W., Clarke, M.F., 2007. Cancer stem cells: models and concepts. Annual Review of Medicine 58, 267–284.

Downing, S., Chien, M.B., Kass, P.H., Moore, P.E., London, C.A., 2002. Prevalence and importance of internal tandem duplications in exons 11 and 12 of c-kit in mast cell tumors of dogs. American Journal of Veterinary Research 63, 1718–1723.

Galli, S.J., Kalesnikoff, J., Grimbaldeston, M.A., Piliponsky, A.M., Williams, C.M., Tsai, M., 2005. Mast cells as "tunable" effector and immunoregulatory cells: recent advances. Annual Review of Immunology 23, 749–786.

Garcia, G., Brazis, P., Majo, N., Ferrer, L., de Mora, F., Puigdemont, A., 1998. Comparative morphofunctional study of dispersed mature canine cutaneous mast cells and BR cells, a poorly differentiated mast cell line from a dog subcutaneous mastocytoma. Veterinary Immunology and Immunopathology 62, 323–337.

Gilfillan, A.M., Tkaczyk, C., 2006. Integrated signalling pathways for mast-cell activation. Nature Review of Immunology 6, 218–230.

Gould, H.J., Sutton, B.J., Beavil, A.J., Beavil, R.L., McCloskey, N., Coker, H.A., Fear, D., Smurthwaite, L., 2003. The biology of IGE and the basis of allergic disease. Annual Review of Immunology 21, 579–628.

Ishiguro, T., Kadosawa, T., Mori, K., Takagi, S., Okumura, M., Fujinaga, T., 2001. Establishment and characterization of a new canine mast cell tumor cell line. The Journal of Veterinary Medical Science 63, 1031–1034.

Kambe, N., Kambe, M., Kochan, J.P., Schwartz, L.B., 2001. Human skin-derived mast cells can proliferate while retaining their characteristic functional and protease phenotypes. Blood 97, 2045–2052.

Liao, A.T., Chien, M.B., Shenoy, N., Mendel, D.B., McMahon, G., Cherrington, J.M., London, C.A., 2002. Inhibition of constitutively active forms of mutant kit by multitargeted indolinone tyrosine kinase inhibitors. Blood 100, 585–593.

Lin, T.Y., Rush, L.J., London, C.A., 2006. Generation and characterization of bone marrow-derived cultured canine mast cells. Veterinary Immunology and Immunopathology 113, 37–52.

London, C.A., Galli, S.J., Yuuki, T., Hu, Z.Q., Helfand, S.C., Geissler, E.N., 1999. Spontaneous canine mast cell tumors express tandem duplications in the proto-oncogene c-kit. Experimental Hematology 27, 689–697.

London, C.A., Seguin, B., 2003. Mast cell tumors in the dog. The Veterinary Clinics of North America: Small Animal Practice 33, 473–489 v.

Ma, Y., Longley, B.J., Wang, X., Blount, J.L., Langley, K., Caughey, G.H., 1999. Clustering of activating mutations in c-KIT's juxtamembrane coding region in canine mast cell neoplasms. The Journal of Investigative Dermatology 112, 165–170.

Ma, Y., Zeng, S., Metcalfe, D.D., Akin, C., Dimitrijevic, S., Butterfield, J.H., McMahon, G., Longley, B.J., 2002. The c-KIT mutation causing human mastocytosis is resistant to STI571 and other KIT kinase inhibitors; kinases with enzymatic site mutations show different inhibitor sensitivity profiles than wild-type kinases and those with regulatory-type mutations. Blood 99, 1741–1744.

Momoi, Y., Okai, Y., Watari, T., Goitsuka, R., Tsujimoto, H., Hasegawa, A., 1997. Establishment and characterization of a canine T-lymphoblastoid cell line derived from malignant lymphoma. Veterinary Immunology and Immunopathology 59, 11–20.

Ohmori, K., Maeda, S., Okayama, T., Masuda, K., Ohno, K., Tsujimoto, H., 2004. Molecular cloning of canine activation-induced cytidine deaminase (AID) cDNA and its expression in normal tissues. The Journal of Veterinary Medical Science 66, 739–741.

Patnaik, A.K., Ehler, W.J., MacEwen, E.G., 1984. Canine cutaneous mast cell tumor: morphologic grading and survival time in 83 dogs. Veterinary Pathology 21, 469–474.

Pryer, N.K., Lee, L.B., Zadovaskaya, R., Yu, X., Sukbuntherng, J., Cherrington, J.M., London, C.A., 2003. Proof of target for SU11654: inhibition of KIT phosphorylation in canine mast cell tumors. Clinical Cancer Research 9, 5729–5734.

Roskoski Jr., R., 2005a. Signaling by Kit protein-tyrosine kinase—the stem cell factor receptor. Biochemical and Biophysical Research Communications 337, 1–13.

Roskoski Jr., R., 2005b. Structure and regulation of Kit protein-tyrosine kinase—the stem cell factor receptor. Biochemical and Biophysical Research Communications 338, 1307–1315.

Takahashi, T., Kitani, S., Nagase, M., Mochizuki, M., Nishimura, R., Morita, Y., Sasaki, N., 2001. IgG-mediated histamine release from canine mastocytoma-derived cells. International Archives of Allergy and Immunology 125, 228–235.

Tsai, K.L., Guyon, R., Murphy, K.E., 2003. Identification of isoforms and RH mapping of canine KIT. Cytogenetic and Genome Research 102, 261–263.

Yarden, Y., Kuang, W.J., Yang-Feng, T., Coussens, L., Munemitsu, S., Dull, T.J., Chen, E., Schlessinger, J., Francke, U., Ullrich, A., 1987. Human proto-oncogene c-kit: a new cell surface receptor tyrosine kinase for an unidentified ligand. The EMBO Journal 6, 3341–3351.

Zemke, D., Yamini, B., Yuzbasiyan-Gurkan, V., 2002. Mutations in the juxtamembrane domain of c-KIT are associated with higher grade mast cell tumors in dogs. Veterinary Pathology 39, 529–535.

Zermati, Y., De Sepulveda, P., Feger, F., Letard, S., Kersual, J., Casteran, N., Gorochov, G., Dy, M., Ribadeau Dumas, A., Dorgham, K., Parizot, C., Bieche, Y., Vidaud, M., Lortholary, O., Arock, M., Hermine, O., Dubreuil, P., 2003. Effect of tyrosine kinase inhibitor STI571 on the kinase activity of wild-type and various mutated c-kit receptors found in mast cell neoplasms. Oncogene 22, 660–664.

APPLIED AND ENVIRONMENTAL MICROBIOLOGY, Nov. 2008, p. 6538–6546 Vol. 74, No. 21
0099-2240/08/$08.00+0 doi:10.1128/AEM.01354-08

Codon Optimization Increases Steady-State mRNA Levels in *Aspergillus oryzae* Heterologous Gene Expression▽†

Masafumi Tokuoka,[1]‡ Mizuki Tanaka,[1] Kazuhisa Ono,[2] Shinobu Takagi,[3] Takahiro Shintani,[1] and Katsuya Gomi[1]*

Laboratory of Bioindustrial Genomics, Department of Bioindustrial Informatics and Genomics, Graduate School of Agricultural Science, Tohoku University, 1-1 Tsutsumidori-Amamiyamachi, Aoba-ku, Sendai 981-8555, Japan[1]; Department of Molecular Biotechnology, Graduate School of Advanced Sciences of Matter, Hiroshima University, 1-3-1 Kagamiyama, Higashi-Hiroshima 739-8530, Japan[2]; and Novozymes Japan Ltd., CB-6, Makuhari Techno Garden, 1-3 Nakase, Mihama-ku, Chiba 261-8501, Japan[3]

Received 17 June 2008/Accepted 3 September 2008

We investigated the effect of codon optimization on the expression levels of heterologous proteins in *Aspergillus oryzae*, using the mite allergen Der f 7 as a model protein. A codon-optimized Der f 7 gene was synthesized according to the frequency of codon usage in *A. oryzae* by recursive PCR. Both native and optimized Der f 7 genes were expressed under the control of a high-level-expression promoter with their own signal peptides or in a fusion construct with *A. oryzae* glucoamylase (GlaA). Codon optimization markedly increased protein and mRNA production levels in both nonfused and GlaA-fused Der f 7 constructs. For constructs with native codons, analysis by 3′ rapid amplification of cDNA ends revealed that poly(A) tracts tended to be added within the coding region, producing aberrant mRNAs that lack a termination codon. Insertion of a termination codon between the carrier GlaA and native Der f 7 proteins in the GlaA fusion construct resulted in increases in mRNA and secreted-carrier-GlaA levels. These results suggested that mRNAs without a termination codon as a result of premature polyadenylation are degraded, possibly through the nonstop mRNA decay pathway. We suggest that codon optimization in *A. oryzae* results in elimination of cryptic polyadenylation signals in native Der f 7, thereby circumventing the production of truncated transcripts and resulting in an increase in steady-state mRNA levels.

The filamentous fungus *Aspergillus oryzae* has been used in the production of fermented foods, such as sake, soy sauce, and miso (soybean paste), in Japan for over a thousand years. In addition, *A. oryzae* has the ability to secrete large amounts of proteins and has recently become a favorable host for recombinant protein production (5). By use of a series of classical random mutagenesis and screening procedures, hypersecretion mutants of heterologous proteins in aspergilli have been obtained (9, 49). However, the secretion yields of heterologous proteins are low compared to those of homologous proteins or proteins from closely related fungal species and generally do not exceed tens of milligrams per liter (16). In order to improve the expression levels of heterologous proteins, several trials have been conducted, and some strategies have been reported to be effective in increasing the level of heterologous protein production (39). These results provide information on how to increase the expression levels of heterologous genes; however, there is little information on the mechanisms hampering heterologous gene expression. In this study, we investigate the effect of codon optimization on heterologous gene expression. Such optimization has been effective in improving secretion levels of heterologous proteins in several hosts (19). Studies of heterologous gene expression through codon optimization have reported improved heterologous protein production in filamentous fungal species, such as *Aspergillus awamori* (2, 15, 35), *Aspergillus niger* (27, 35), *Neurospora crassa* (13, 35), and *Trichoderma reesei* (47). Based on studies of bacteria, codon optimization is believed to improve translational efficiency, resulting in increased levels of protein production (4, 22, 25). Also, some studies of filamentous fungi have indicated that codon optimization increased mRNA levels, resulting in increased protein production (15, 27, 41, 47). Regardless, there is little information on the mechanism by which codon optimization increases the expression levels of heterologous genes in filamentous fungi. To elucidate such mechanisms in *A. oryzae*, we used Der f 7 as a model heterologous protein. Der f 7, a secretion protein of the house dust mite *Dermatophagoides farinae*, belongs to the group 7 mite allergens that react with immunoglobulin E in 50% of patients allergic to house dust (26, 43). House dust allergy is a serious problem among all allergic diseases, and specific allergens are required for diagnostics and immunotherapy. Allergens prepared from mites generally contain irrelevant proteins and can cause undesirable immune responses. Therefore, recombinant allergens present an attractive alternative to mite extracts. For clinical purposes, it is of great importance to prepare large quantities of specific recombinant allergens (3). Therefore, there have been many attempts to produce large quantities of mite allergen proteins by using *Escherichia coli* (54), *Saccharomyces cerevisiae* (6), *Pichia pastoris* (23, 53), and *A. oryzae*

* Corresponding author. Mailing address: Laboratory of Bioindustrial Genomics, Department of Bioindustrial Informatics and Genomics, Graduate School of Agricultural Science, Tohoku University, 1-1 Tsutsumidori-Amamiyamachi, Aoba-ku, Sendai 981-8555, Japan. Phone: 81-22-717-8901. Fax: 81-22-717-8902. E-mail: gomi@biochem.tohoku.ac.jp.

‡ Present address: Noda Institute of Industrial Sciences, 399 Noda, Noda 278-0037, Japan.

† Supplemental material for this article may be found at http://aem.asm.org/.

▽ Published ahead of print on 12 September 2008.

TABLE 1. Oligonucleotides used for total synthesis of the codon-optimized Der f 7 gene

Oligonucleotide no.	Sequence (5′→3′)
1	5′-CCCGTCGACCATGATGAAGTTCTTGCT GATCGCTGCCGTCGCCTTCGTCGCCGT TTCGGCTGACCCCATTCACTACGACAA GATCACCGAGGAAATCAACAAGGCTA TCG-3′[a]
2	5′-ACGCTCGAACTTGTCGGCGTGGTCAG GGACCTTCATGGGATCGATGGTCTCG GACTGTTCGATAGCAGCAATGGCATC GTCGATAGCCTTGTTGATTT-3′
3	5′-CGACAAGTTCGAGCGTCACGTTGGTA TCGTGGACTTCAAGGGTGAGTTGGCC ATGCGCAACATCGAGGCTCGCGGCCT CAAGCAGATGAAGCGTCA-3′
4	5′-TCGACACGATATCATCGTGAACACCG ATGAGCAAATGAGCCTTAACAATACC CTCTTCACCCTTGACATTAGCGTCACC CTGACGCTTCATCTGCTT-3′
5	5′-CGATGATATCGTGTCGATGGAGTACG ATCTCGCCTACAAGCTGGGTGACCTTC ATCCCACCACTCACGTCATCTCGGATA TTCAGGACTTCGT-3′
6	5′-TGACAACATTAGCGAATTGGCGGACC TCGAAAGAGGTCATGGTGATGTTACC TTCGTCAGAAATCTCAAGGGAGAGGG CAACAACGAAGTCCTGAATATC-3′
7	5′-CAATTCGCTAATGTTGTCAACCACATC GGTGGCCTTTCCATCCTCGACCCCATT TTCGGCGTTCTCTCTGATGTCCTGACC GCTATCTTCCAAGACACCG-3′
8	5′-CCCTCTAGATTAATTCTTTTCCAGCTC ACGCTTGAAGGCGGGGGCCAGGACCT TGGTCATTTCCTTACGGACGGTGTCTT GGAAGATAG-3′[b]

[a] The SalI site is underlined.
[b] The XbaI site is underlined.

(44) as microbial hosts. With respect to these attempts, recombinant Der f 1 produced in *A. oryzae* has been reported to have immunoglobulin E-binding activity similar to that of native Der f 1, while recombinant Der f 1 produced in bacteria had weaker binding activity than native Der f 1 (44). These results suggested that *A. oryzae* is a suitable host for production of Der f 7 for immunotherapy.

MATERIALS AND METHODS

Strains, culture conditions, and DNA preparation. *A. oryzae* NS4 (52) was used as a recipient strain for transformation. *E. coli* DH5α (*supF44 hsdR17 recA1 endA1 gyrA96 thi-1 relA1 lacU169* Φ80*lac*ZM15) was used for construction and propagation of plasmid DNAs. Czapek-Dox medium, containing 1% glucose, 0.3% $NaNO_3$, 0.15% KCl, 0.1% KH_2PO_4, 0.05% $MgSO_4$, and 0.1% methionine, was used as a selective medium for fungal transformation. For protein expression, YPM medium, containing 1% yeast extract, 2% peptone, and 2% maltose, was used. Transformation of *A. oryzae* was performed by the methods of Gomi et al. (12), and DNA manipulation and propagation were performed using standard DNA techniques (40).

Construction of a synthetic Der f 7 gene. A codon-optimized Der f 7 gene was synthesized by PCR using eight mutually priming, overlapping oligonucleotides which were designed based on the *A. oryzae* codon usage database (http://www.kazusa.or.jp/codon/) (Table 1). Recursive PCR (1, 38) was performed using Ex-*Taq* polymerase (Takara Bio, Otsu, Japan) under the following reaction conditions: 30 cycles of denaturation at 94°C for 60 s, annealing at 60°C for 60 s, and elongation at 72°C for 60 s. The first PCR product was used as a template for the second PCR, which was performed under the same conditions, using the 3′ and 5′ terminal oligonucleotides as primers. The resulting product was cloned into a pCRII-TOPO cloning vector (Invitrogen, Tokyo, Japan) and subjected to DNA sequencing to select a clone containing the designed codon-optimized Der f 7 gene. The DNA cycle sequencing reaction was performed with a universal sequencing primer, using a Big-Dye Terminator 3.1 cycle sequencing kit (Applied Biosystems, Foster City, CA) with an ABI PRISM 377 sequencer (Applied Biosystems). The plasmid clone pTDopt, containing a designed nucleotide sequence, was used in further study as the codon-optimized Der f 7 gene.

Construction of expression vectors. The Der f 7 gene with native codons and an original signal sequence was amplified by PCR on pGEX-Der f 7 (a gift from S. Kawamoto, Hiroshima University), using primers 5′-CCCGTCGACATGAT GAAATTTTGTTGAT-3′ (the SalI restriction site is underlined) and 5′-CCC TCTAGATTAATTTTTTTCCAATTCAC-3′ (the XbaI restriction site is underlined). An amplified fragment was inserted between the improved *glaA* promoter and the *agdA* terminator of an expression vector, pNGA142 (46), which contains the *niaD* gene as a selectable marker, yielding pDer/ntv. The Der f 7 gene fragment with optimized codons, obtained by digestion of pTDopt with XbaI and SalI, was also cloned into XbaI/SalI-digested pNGA142, yielding pDer/opt.

pGlaDer/ntv and pGlaDer/opt were constructed based on pNGL, which contains a glucoamylase A (GlaA) catalytic domain region in the NotI and PmaCI sites of pNGA142. A DNA fragment encoding the GlaA catalytic domain was prepared by PCR with *A. oryzae* genomic DNA by using primers 5′-CCCGCG GCCGCATGGTGTCTTTCTCCTCTTG-3′ (the NotI restriction site is underlined) and 5′-CCCCACGTGAGTCGTAGAGCAAGCTGACG-3′ (the PmaCI restriction site is underlined) and was inserted into NotI/PmaCI-digested pNGA142, resulting in pNGL. The Der f 7 gene without a signal sequence was amplified by PCR using the following primers: 5′-CCCCACGTG*AAAAGA*GA TCCAATTCACTATGATAA-3′ (the PmaCI restriction site is underlined) and 5′-CCCATATGTTGGTTTTTTTCCAATTCACG-3′ (the NdeI restriction site is underlined) for the native-codon construct and 5′-CCCCACGTG*AAACGC*G ACCCCATTCACTACGACAA-3′ (the PmaCI restriction site is underlined) and 5′-CCCCATATGTTAATTCTTTTCCAGCTCAC-3′ (the NdeI restriction site is underlined) for the codon-optimized construct. Both sense primers contained hexanucleotides encoding a cleavage site (shown in italics) for a Kexin-like protease (KexB) (34), Lys-Arg. PCR-amplified fragments were inserted in the PmaCI and NdeI sites of pNGL to be fused in-frame at the 3′ terminus of the nucleotide sequence encoding the GlaA catalytic domain through the KexB cleavage sequence Lys-Arg.

pGlaDer/ntv-stop was constructed by deletion of two nucleotides (5′-CG-3′) located immediately upstream of the KexB cleavage site of the GlaA::Der f 7 fusion. That created a frameshift and a termination codon occurring 8 codons after the deletion site.

SDS-PAGE and Western blot analysis. Proteins secreted by transformants cultured in YPM medium for 24 h were analyzed by sodium dodecyl sulfate-polyacrylamide gel electrophoresis (SDS-PAGE) (30) on 12.5% polyacrylamide gels and strained with Coomassie brilliant blue (CBB) R-250. Proteins in the medium samples were concentrated by precipitation with 10% trichloroacetic acid (TCA). For Western analysis, 20 μl of culture medium was electrophoresed and transferred onto a polyvinylidene difluoride membrane (Nippon Genetics, Tokyo, Japan) by using a semidry blotting system (Bio-Rad, Hercules, CA) with 3-(cyclohexylamino)-1-propanesulfonic acid buffer. Membranes were incubated with rabbit anti-Der f 7 polyclonal antibody and then detected with an immunostaining kit (Konica, Tokyo, Japan), using peroxidase-conjugated goat-rabbit antibodies (Promega, Madison, WI).

Quantitative RT-PCR analysis. Total RNAs were extracted from mycelia of transformants cultured for 20 h at 30°C using Isogen (Nippon Gene, Tokyo, Japan) according to the manufacturer's instructions. Five micrograms of total RNA was treated with DNase I (Nippon Gene), and first-strand cDNAs were synthesized using murine leukemia virus reverse transcriptase (Invitrogen) with an oligo(dT) primer. Synthesized cDNA was treated with RNase H, and quantitative reverse transcription-PCR (RT-PCR) was performed with DyNAmo (Finnzymes, Espoo, Finland), using the following primers: for the native-codon Der f 7 gene, 5′-CGTGGCTTCTTCTACACACCC-3′ (forward) and 5′-AGCT CCAGTTGTGCCACTTGT-3′ (reverse); for the codon-optimized Der f 7 gene, 5′-GACGATGCCATTGCTGCTAT-3′ (forward) and 5′-ACACCGATGAGCA AATGAGC-3′ (reverse); and for the histone gene, 5′-CAAGCGTATCTCTGC CATGA-3′ (forward) and 5′-CACCGAAACCGTAGAGGGTA-3′ (reverse). Reactions and subsequent analyses were performed with the DNA Engine Opticon system (MJ Research, San Francisco, CA). The relative mRNA levels were normalized to that of the histone H4 gene, used as a reference gene (33).

Northern blot analysis. A digoxigenin (DIG)-labeled double-strand DNA probe was synthesized on pDer/ntv-opt as a template by using a PCR DIG probe kit (Roche, Indianapolis, IN). Five micrograms of total RNA was electropho-

rested on a 1.5% formaldehyde-agarose gel. RNA quality was evaluated by visualization of rRNA stained with ethidium bromide. Transfer of the total RNAs onto a Hybond N+ nylon membrane (Amersham Biosciences, Amersham, United Kingdom), prehybridization, and hybridization were performed according to the DIG luminescence kit protocol (Roche). Signal detection was performed with CSPD (Roche) as a substrate, according to the manufacturer's instructions, before exposure to X-ray film (Fuji Film, Tokyo, Japan).

3′-RACE analysis and poly(A) addition site mapping. The polyadenylation sites of Der f 7 mRNAs from Der/ntv and Der/opt were mapped using analysis by 3′ rapid amplification of cDNA ends (3′-RACE). Approximately 5 μg of total RNA, prepared for Northern blot analysis as described above, was used for cDNA synthesis using a GeneRacer kit (Invitrogen). PCR amplification was performed using the sense primers (5′-CCCCACGTGAAAAGAGATCCAATTCACTATGATAA-3′ for native Der f 7 and 5′-CCCCACGTGAAACGCGACCCCATTCACTACGACAA-3′ for codon-optimized Der f 7) used for amplification of the Der f 7 gene for the fusion construct and the antisense primer supplied with the kit. Amplified products were inserted into a pCRII-TOPO cloning vector (Invitrogen), and the resulting plasmids were digested with EcoRI, followed by agarose electrophoresis to compare the inserted fragment lengths of the obtained clones. The DNA cycle sequencing reaction was performed as described above.

Nucleotide sequence accession number. The nucleotide sequence of the codon-optimized Der f 7 gene constructed in this study has been deposited in the DDBJ/GenBank/EMBL databases under accession number AB441028.

RESULTS

Design and construction of codon-optimized Der f 7. Comparison of the codon usage of Der f 7 with that of *A. oryzae* by use of a codon usage database (http://www.kazusa.or.jp/codon/) showed that the frequencies of individual codons are different from those in *A. oryzae*. The GC content of the coding region of native Der f 7 was 37.8%, while that of *A. oryzae* genes is ≈55% (http://www.kazusa.or.jp/codon/). Based on codon usage, a codon-optimized Der f 7 gene was designed. Codons infrequently used in *A. oryzae* were replaced by more-frequently used codons, and portions of other codons were altered to reflect the usage of individual codons (Table 2). Consequently, 43.7% of the codons in native Der f 7 were altered. Reconstitution of the gene by codon optimization resulted in a GC content of 52.8%.

The codon-optimized Der f 7 gene was synthesized in two rounds of recursive PCR (1, 38). The resulting PCR products were cloned, and 1 clone, whose sequence corresponded to the designed codon-optimized Der f 7 gene, was obtained out of 15 clones. Using the native Der f 7 gene and the synthesized, codon-optimized Der f 7 gene, we constructed Der f 7 expression vectors pDer/ntv and pDer/opt. These contained the Der f 7 gene that was inserted downstream of the improved *glaA* promoter (46). In addition, we constructed the expression vectors pGlaDer/ntv (for native Der f 7) and pGlaDer/opt (for codon-optimized Der f 7) to evaluate the effect of codon optimization in the fusion construct. Der f 7 without a signal sequence was fused to the catalytic domain of *A. oryzae* GlaA at the N terminus through a KexB cleavage site. Both types of expression vectors were constructed based on a fungal high-level-expression vector, pNGA142 (46).

A. oryzae NS4 was transformed using the above-mentioned vectors. Transformants containing one copy of an expression vector at the resident *niaD* locus as determined by Southern blot analysis (data not shown) were selected. Two independent transformants were selected for further analysis in individual transformation experiments.

TABLE 2. Comparison of codon usage in *A. oryzae* genes with that in native and codon-optimized Der f 7 genes

Amino acid	Codon	% Frequency[a]		
		A. oryzae	Der f 7	
			Native	Optimized
Ala	GCT	27	50	50
	GCC	31	30	50
	GCA	23	20	0
	GCG	20	0	0
Arg	CGT	18	58	58
	CGC	23	0	42
	CGA	17	42	0
	CGG	18	0	0
	AGA	13	0	0
	AGG	12	0	0
Asn	AAT	45	58	58
	AAC	55	42	42
Asp	GAT	53	94	36
	GAC	47	6	64
Cys	TGT	46	0	0
	TGC	54	0	0
Gln	CAA	43	100	32
	CAG	57	0	68
Glu	GAA	44	88	38
	GAG	56	12	62
Gly	GGT	28	82	74
	GGC	31	9	26
	GGA	24	9	0
	GGG	17	0	0
His	CAT	47	76	24
	CAC	53	24	76
Ile	ATT	36	67	29
	ATC	50	24	71
	ATA	14	9	0
Leu	TTA	7	17	0
	TTG	18	65	17
	CTT	19	17	17
	CTC	23	0	36
	CTA	11	0	0
	CTG	22	0	29
Lys	AAA	36	93	0
	AAG	64	7	100
Met	ATG	100	100	100
Phe	TTT	38	60	0
	TTC	62	40	100
Pro	CCT	27	18	18
	CCC	26	0	82
	CCA	25	82	0
	CCG	22	0	0
Ser	AGT	13	0	0
	AGC	18	0	0
	TCT	18	33	33
	TCC	20	22	33
	TCA	14	12	0
	TCG	16	33	33
Thr	ACT	24	12	12
	ACC	32	55	88
	ACA	24	33	0
	ACG	20	0	0
Trp	TGG	100	100	100
Tyr	TAT	47	69	0
	TAC	53	31	100
Val	GTT	27	40	40
	GTC	33	25	50
	GTA	13	25	0
	GTG	27	10	10

[a] Percent frequencies of individual codons are shown for each corresponding amino acid.

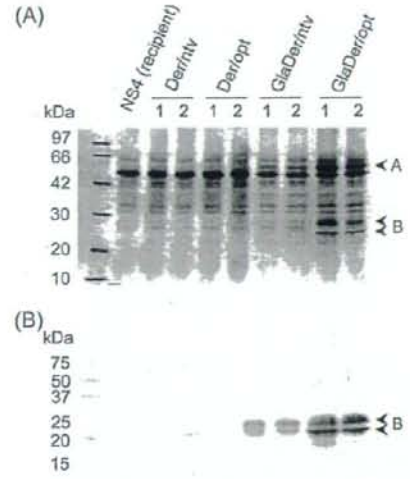

FIG. 1. SDS-PAGE analysis of the transformants. (A) CBB staining. (B) Western blotting. Two independent transformants harboring a single copy of each expression cassette were grown in YPM medium for 24 h at 30°C. The culture supernatant (100 μl) concentrated fivefold by precipitation with TCA was loaded on a 12.5% SDS-polyacrylamide gel. Anti-Der f 7 antibodies were used for Western blotting. Arrowheads designated A and B indicate the carrier GlaA protein and Der f 7, respectively.

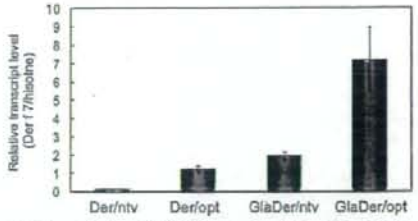

FIG. 2. Quantitative RT-PCR analysis of Der f 7 mRNAs in the transformants. Total RNAs were extracted from transformant mycelia grown in YPM medium for 24 h. cDNAs were subjected to real-time PCR analysis using specific primers as described in Materials and Methods. The relative expression level for each gene was normalized to that for the histone H4 gene. The values are means of results from three independent experiments, and the error bars denote standard errors.

Codon optimization improves Der f 7 production in nonfused and fused constructs. To investigate the effect of codon optimization on protein production levels, the transformants and the parental strain were cultured, and the culture supernatants were subjected to SDS-PAGE analysis. CBB staining showed that α-amylase signals of around 55 kDa were similar in all samples, indicating no difference in protein production ability among the transformants. Western blot analysis showed that two signals, of ≈25 and 30 kDa, were detected in the culture supernatants of transformants Der/opt-1 and -2 (Fig. 1B). In contrast, no signals were detected in those of transformants Der/ntv-1 and -2. This result indicates that codon optimization increased the amount of secreted Der f 7 from an undetectable level to a detectable level in the nonfused construct.

In the fusion constructs, two distinct signals, of ≈25 and 30 kDa, were detected by Western blot analysis in the culture supernatants of transformants GlaDer/opt-1 and -2, whereas weaker signals were detected in those of transformants GlaDer/ntv-1 and -2 (Fig. 1B). Signal intensity quantification of the bands by use of NIH image software (National Institutes of Health, Bethesda, MD) indicated that the signal intensities of the GlaDer/opt band were three- to fivefold higher than those of GlaDer/ntv. In addition, protein bands corresponding to the signals detected by Western blot analysis were observed only in the culture supernatants of transformants GlaDer/opt-1 and -2 by CBB staining (Fig. 1A and B). Furthermore, bands of ≈60 kDa, corresponding to the size of the catalytic domain of GlaA, were detected in both GlaDer/ntv and GlaDer/opt (Fig. 1A), although the signal intensity of the band in GlaDer/ntv was noticeably weak. Compared with the result for the nonfused construct, the fusion strategy markedly increased secretion yields of Der f 7 in both the native and the codon-optimized constructs. However, secretion yield in GlaDer/opt was much higher than that in GlaDer/ntv, indicating that codon optimization might synergistically improve production of Der f 7 when a fusion strategy is employed.

In this study, the nucleotide sequence around the start codon did not follow Kozak's rule in the fusion constructs (the NotI site of the primer contains a "C" at position −3 relative to the AUG codon). This structure might be expected to negatively affect translation efficiency (29). However, because both pGlaDer/ntv and pGlaDer/opt had the same sequence at position −3, the translation efficiencies in the two constructs were not expected to differ from each other. Additionally, the amount of recombinant Der f 7 produced in GlaDer/opt was much higher (>5-fold) than that in Der/opt, which has a "G" at position −3 (Fig. 1). The ratio of steady-state mRNA levels between GlaDer/opt and Der/opt was ≈5-fold (Fig. 2) (see below). These observations were associated with the positive effect of GlaA, the carrier protein fused to Der f 7, but these results suggested that the sequence around the start codon did not significantly affect the translation efficiency.

SDS-PAGE analysis of mite Der f 7 indicated that two bands, of 30 and 31 kDa, were glycosylated forms of a 25-kDa protein (43). The medium sample of the transformants was treated with endoglycosidase H, confirming that the 30-kDa band was a glycosylated form of the 25-kDa protein (data not shown).

Comparison of the Der f 7 mRNA levels. To investigate whether differences in secretion yields of Der f 7 between transformants containing codon-optimized Der f 7 and those containing native Der f 7 could be explained at the transcriptional level, Der f 7 mRNA levels in each transformant were compared by quantitative RT-PCR analysis. Total RNAs were extracted from the transformants cultivated in YPM medium for 20 h. Transformants containing the codon-optimized Der f 7 gene (Der/opt or GlaDer/opt) had higher Der f 7 mRNA levels than transformants containing the native-codon Der f 7 gene (Der/ntv or GlaDer/ntv) (Fig. 2). The Der f 7 mRNA level of transformant Der/opt was ≈10-fold higher than that of

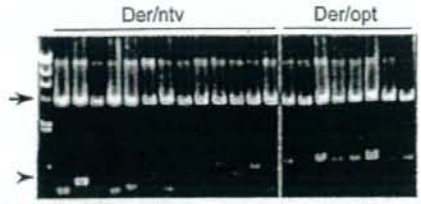

FIG. 3. Analysis of the inserted fragments of two 3′-RACE clones. First-strand cDNA was synthesized using an oligo(dT) anchor primer. Then, PCR was performed using the anchor primer and the Der f 7-specific primer, and amplified PCR fragments were cloned by insertion into the pCRII TA-cloning vector. The resulting plasmid DNAs were isolated and digested with EcoRI, followed by agarose gel electrophoresis to compare the lengths of the inserted fragments. The arrow indicates the bands of the TA-cloning vector used for cloning of the RT-PCR products, and the arrowhead indicates a 500-bp molecular marker.

transformant Der/ntv. Similarly, that of transformant GlaDer/opt was ≈3- to 5-fold higher than that of GlaDer/ntv. These data suggested that codon optimization increased the steady-state mRNA level, resulting in significant improvement of the secretion yield of Der f 7.

3′-RACE analysis and polyadenylation site mapping. As described above, codon optimization of Der f 7 could be effective for improving mRNA transcript yield and could result in an increase in protein production level. However, the precise mechanism by which codon optimization increased the expression level of the heterologous gene was unclear. Because truncation of mRNA has been reported to occur in heterologous gene expression in filamentous fungi (14, 15, 42), we examined the lengths of Der f 7 transcripts by RT-PCR and then sequenced the amplified products in transformants Der/ntv and Der/opt.

RT-PCR was performed using the total RNAs used for Northern analysis as described above. RT-PCR products were cloned with the TA-cloning system, and clones were arbitrarily selected to be digested with EcoRI prior to agarose gel electrophoresis. The Der f 7 cDNA fragments in Der/opt were mostly uniform in length, whereas those in Der/ntv were shorter and varied considerably (Fig. 3). This suggested that expression of the Der f 7 construct with native codons results in formation of truncated mRNAs and that codon optimization prevents truncation of transcripts. Further DNA sequencing of amplified fragments revealed that multiple polyadenylation sites were located within the coding region but not in the 3′ untranslated region in the construct pDer/ntv. Yet, polyadenylation sites occurred within the 3′ untranslated region in all cDNA clones examined in the construct pDer/opt (Fig. 4). In addition, premature termination of transcription occurred in the fusion construct pGlaDer/ntv (see Fig. S1 in the supplemental material). These results suggest that formation of aberrant mRNA without a termination codon is correlated with mRNA levels.

Translation termination codon insertion upstream of Der f 7. As described above, we showed that expression of the heterologous gene with high-level AT content resulted in truncation of the transcripts and that codon optimization could prevent formation of such aberrant mRNAs, possibly by eliminating AT-rich sequences. Premature polyadenylation within the coding region forms truncated mRNA without a translational termination codon, the so-called nonstop mRNA. Recently, the nonstop mRNA decay pathway was proposed as the mechanism underlying the correlation between premature polyadenylation and decreased mRNA levels (10, 48). This pathway is thought to play a role in the quality control of mRNAs. mRNAs that lack a translational termination codon are degraded through the pathway to prevent the synthesis of potentially deleterious proteins from aberrant mRNAs. Der f 7 mRNAs containing a premature poly(A) tract within the coding region have no in-frame translation termination codon. We therefore presumed that Der f 7 mRNAs are rapidly degraded through the nonstop mRNA decay pathway in the construct pDer/ntv.

It has been reported that transcript degradation was avoided

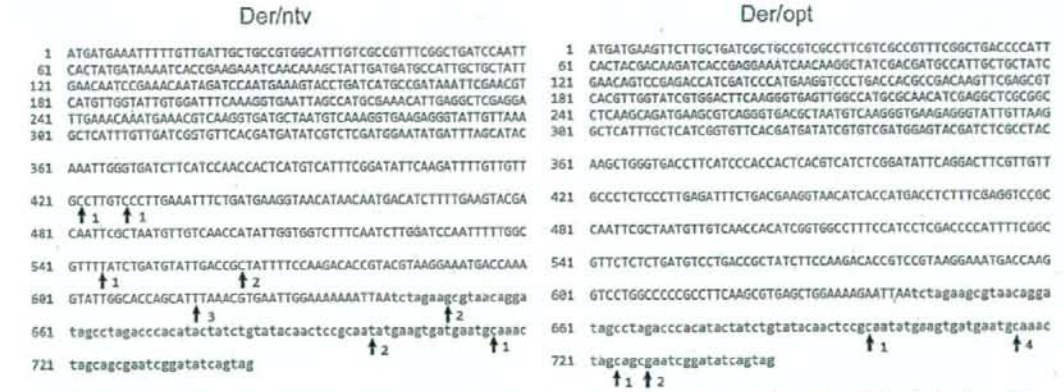

FIG. 4. Polyadenylation sites of Der f 7 mRNA in the transformants Der/ntv and Der/opt. Arrows indicate the polyadenylation sites of the two sequenced 3′-RACE clones. The nucleotide sequence of the coding region is indicated in uppercase letters, and the terminator sequence is indicated in lowercase letters. Numbers beside the arrow indicate the number of clones containing the poly(A) tract at the indicated position.

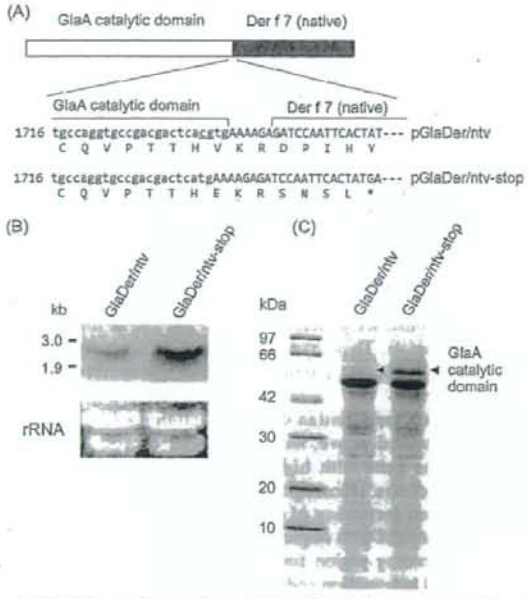

FIG. 5. Expression analysis of GlaA::Der f 7 fusion genes with or without a premature termination codon. (A) Nucleotide and amino acid sequences around the fused region of pGlaDer/ntv and pGlaDer/ntv-stop. Two deleted nucleotides are underlined. (B) Northern blot analysis. Total RNAs were extracted from transformant mycelia cultured in YPM medium for 24 h using the native Der f 7 gene as a probe. (C) CBB staining of SDS-polyacrylamide gel. Culture supernatants of 24-h-grown transformants were concentrated fivefold by TCA precipitation, followed by SDS-PAGE. Arrowheads indicate the protein band corresponding to the GlaA catalytic domain.

by the addition of a translation termination codon upstream of the poly(A) tract in nonstop gene constructs (10). If Der f 7 mRNAs were degraded through such a nonstop mRNA decay pathway, insertion of a termination codon upstream of the polyadenylation site would increase the Der f 7 mRNA level. Premature polyadenylation occurred in the fusion construct pGlaDer/ntv as well as in the direct construct pDer/ntv. Therefore, we constructed a frameshift mutant of the fusion construct (pGlaDer/ntv-stop) in which the translation termination codon was located downstream of the GlaA catalytic domain. Schematic diagrams of the Der f 7 genes of pGlaDer/ntv and pGlaDer/ntv-stop and their sequence alignment are shown in Fig. 5. These two constructs were introduced into *A. oryzae*, and the mRNA levels were determined by Northern blot analysis. The mRNA level of the fusion gene increased by ≈2- to 3-fold by occurrence of a translational termination codon between *glaA* and Der f 7 (Fig. 5B), suggesting that the native Der f 7 mRNA is degraded by the nonstop mRNA decay pathway. The fusion constructs pGlaDer/ntv and pGlaDer/ntv-stop produced a protein of ≈60 kDa, corresponding to the GlaA catalytic domain generated by cleavage of GlaA::Der f 7 with a Kexin-like protease or by termination of translation downstream of the catalytic domain. Densitometric analyses following SDS-PAGE of the medium samples showed that the transformant GlaDer/ntv-stop produced the GlaA catalytic domain at a level ≈5-fold higher than that expressed by the transformant GlaDer/ntv (Fig. 5C).

DISCUSSION

Codon optimization has been considered an effective strategy for improving the expression levels of heterologous genes that contain codons rarely used in the host organism (19). In the present study, we demonstrated that reconstituting the mite allergen gene Der f 7 altered to fit *Aspergillus* codon usage could substantially improve the levels of gene expression and protein production for Der f 7 in *A. oryzae*. It has been suggested that codon optimization does not affect transcript levels but can alleviate the translation inefficiency often caused by ribosomal pauses at rare codons interrupting translation elongation (21, 24, 45, 51). In contrast, it has been reported that in bacteria (50), yeast (37), plants (7, 8), mammalian cells (28), and filamentous fungi (15, 27, 41), native heterologous gene transcripts with rare codons were hardly detectable or were small. By codon optimization, however, heterologous gene transcripts were stabilized or became full-length mRNAs. We observed that codon optimization of the Der f 7 gene resulted in significantly increased levels of mRNA in this study, consistent with these observations. However, it could not be ruled out that translational efficiency plays an important part in the increase in Der f 7 production level caused by codon optimization. Truncated transcripts could not be clearly detected in the pDer/ntv or pGlaDer/ntv construct by Northern blot analyses. However, partial codon optimization of Der f 7, in which chimeric genes were constructed by substituting native fragments (≈100 nucleotides [nt]) for the corresponding codon-optimized fragments, resulted in small amounts of transcripts that were shorter than expected (data not shown). This indicates that truncation of the transcripts occurs in the expression of the Der f 7 gene with rare codons for *A. oryzae*. 3′-RACE analysis clearly demonstrated that premature polyadenylation within the coding region of the gene occurred only in the constructs containing native codons. This suggested that cryptic polyadenylation signals exist within the coding region of the native Der f 7 gene.

There are no known experimental data on the 3′-end processing of mRNAs, including for sequences that function as polyadenylation signals in filamentous fungi. However, the regulatory sequences involved in mRNA 3′-end processing have been extensively studied for mammalian (20), yeast (17, 18), and plant (31) cells. Among these, the hexanucleotide AA UAAA or its related sequences (AUUAAA and AAAAAA) situated between 10 and 30 nt upstream of the 3′-end processing site are known to act as a polyadenylation signal. In addition, a near-upstream element (NUE) generally located within 10 nt upstream of the 3′-end processing site has been characterized as U rich (17). According to these observations, consensus sequences related to AAUAAA could also act as polyadenylation signals in *Aspergillus* spp., although other sequences or combinations of those sequences might also act as polyadenylation signals. To identify the canonical sequences that might function as a polyadenylation signal in native Der f 7 mRNA, we examined those sequences upstream of multiple polyadenylation sites in Der f 7 mRNAs. There was

an AAAAAA sequence immediately upstream of the termination codon but no sequences that perfectly matched AAUAAA or AUUAAA. However, because the native Der f 7 gene is a highly AT-biased gene (GC content of 37.8%), several AU-rich sequences are found upstream of multiple polyadenylation sites. These AU-rich sequences might be involved in premature polyadenylation. Furthermore, sequences related to U-rich motifs are found near the poly(A) sites and likely function as a NUE. In contrast, in the codon-optimized Der f 7 gene, AU-rich and U-rich sequences are absent in the coding region. Taken together, the results suggest that the AU-rich and U-rich sequences present in the coding region of native Der f 7 pre-mRNA are involved in incorrect 3′-end processing. It is also suggested that codon optimization eliminates the AU-rich and U-rich sequences and results in the prevention of premature polyadenylation. Further studies of 3′-end processing mechanisms in filamentous fungal groups, including *Aspergillus* spp., is needed to obtain more information on the *cis*-regulatory sequences, such as polyadenylation signals and NUEs.

We observed a correlation between the decreased Der f 7 mRNA level and premature polyadenylation in the pDer/ntv construct. Similar observations have been reported for heterologous gene expression in filamentous fungal species, such as *A. awamori* and *Schizophyllum commune* (15, 41, 42). These results have indicated that premature polyadenylation within a coding region results in the production of unstable, aberrant transcripts that can be degraded rapidly. However, the mechanisms underlying these findings have not been reported. Recently, a novel mRNA surveillance mechanism in eukaryotes that allows recognition and degrading of aberrant transcripts that lack a termination codon was identified (10, 48). This nonstop mRNA decay pathway is reported to remove the aberrant mRNAs without a termination codon that could encode a truncated protein. Therefore, we examined whether the nonstop mRNA decay pathway is involved in the degradation of aberrant Der f 7 mRNA lacking a termination codon. For this purpose, pGlaDer/ntv-stop, a fusion construct with an artificial translational termination codon upstream of the sequence encoding Der f 7, was used. The addition of a termination codon between the GlaA catalytic domain and Der f 7 resulted in increased mRNA levels and a concomitant increase in the amount of GlaA catalytic domain produced. This result indicated that the nonstop mRNA decay pathway could be relevant to the degradation of aberrant transcripts lacking a termination codon in *A. oryzae*. Taken together, these observations suggest a model by which codon optimization increases the mRNA level of the heterologous Der f 7 gene. That is, a portion of the heterologous gene transcripts containing a cryptic polyadenylation signal(s) is prematurely polyadenylated, and the resulting aberrant mRNAs are degraded by the nonstop mRNA decay system. Codon optimization can eliminate the cryptic polyadenylation signals in the coding region and thus result in the production of full-length mRNA. Although it is plausible that native full-length mRNA with rare codons is unstable and degrades rapidly due to its secondary structure and/or translational pausing, we suggest that aberrant transcripts resulting from premature polyadenylation are most likely degraded through the nonstop mRNA decay pathway. The mRNA decay pathway is thought to be conserved among eukaryotes (10), and we conclude that filamentous fungi also have this pathway. However, in the genome sequence databases of *A. oryzae* (32), *Aspergillus nidulans* (11), and *Aspergillus fumigatus* (36), we could not find any gene homologous to *SKI7* that is reported to play an important role in the nonstop mRNA decay pathway in *S. cerevisiae* (48). Therefore, identification of genes encoding the Ski7p homologue or other associate proteins is necessary to clarify the involvement of this pathway in the degradation of aberrant mRNA in *A. oryzae*.

We report that the transcript of the heterologous Der f 7 gene that contains the AT-biased codon is polyadenylated prematurely within the coding region. Multiple cryptic sequence elements in the Der f 7-coding region might be recognized by fungal cells as polyadenylation signals, although precise sequences have not been elucidated. Recognition of these signals appears to be one factor contributing to the low accumulation of full-length Der f 7 transcripts in *A. oryzae*. Altering the codon usage to represent a fungal-preferred codon bias could result in a decrease in the A and T contents of the heterologous genes and eliminate the cryptic polyadenylation signals within the coding region. In addition, we have proposed that the nonstop mRNA decay pathway, involving aberrant mRNAs that lack a termination codon due to gene AT bias, is involved in degrading heterologous gene transcripts in *A. oryzae*.

ACKNOWLEDGMENTS

We thank Seiji Kawamoto for providing the anti-Der f 7 antibody and the plasmid pGEX-Der f 7.

This work was supported in part by a Grant-in-Aid for Scientific Research on Priority Areas, Applied Genomics (no. 17019001), from the Ministry of Education, Culture, Sports, Science and Technology of Japan.

REFERENCES

1. **Brocca, S., C. Schmidt-Dannert, M. Lotti, L. Alberghina, and R. Schmid.** 1998. Design, total synthesis, and functional overexpression of the *Candida rugosa lip1* gene coding for a major industrial lipase. Protein Sci. 7:1415–1422.
2. **Cardoza, R. E., S. Gutierrez, N. Ortega, A. Colina, J. Casqueiro, and J. F. Martin.** 2003. Expression of a synthetic copy of the bovine chymosin gene in *Aspergillus awamori* from constitutive and pH-regulated promoters and secretion using two different pre-pro sequences. Biotechnol. Bioeng. 83: 249–259.
3. **Chapman, M. D., A. M. Smith, L. D. Vailes, and L. K. Arruda.** 1997. Defined epitopes: In vivo and in vitro studies using recombinant allergens. Int. Arch. Allergy Immunol. 125:102–104.
4. **Chen, G. T., and M. Inouye.** 1994. Role of the AGA/AGG codons, the rarest codons in global gene expression in *Escherichia coli*. Genes Dev. 8:2641–2652.
5. **Christensen, T., H. Woeldike, F. Boel, S. B. Mortensen, K. Hjortshoej, L. Thim, and M. Hansen.** 1988. High level expression of recombinant genes in *Aspergillus oryzae*. Bio/Technology 6:1419–1422.
6. **Chua, K. Y., P. K. Kehal, W. R. Thomas, P. R. Vaughan, and I. G. Macreadie.** 1992. High-frequency binding of IgE to the Der p allergen expressed in yeast. J. Allergy Clin. Immunol. 89:95–102.
7. **De Rocher, E. J., T. C. Vargo-Gogola, S. H. Diehn, and P. J. Green.** 1998. Direct evidence for rapid degradation of *Bacillus thuringiensis* toxin mRNA as a cause of poor expression in plants. Plant Physiol. 117:1445–1461.
8. **Diehn, S. H., W.-L. Chin, E. J. De Rocher, and P. J. Green.** 1998. Premature polyadenylation at multiple sites within a *Bacillus thuringiensis* toxin gene-coding region. Plant Physiol. 117:1433–1443.
9. **Dunn-Coleman, N. S., P. Bloebaum, R. M. Berka, E. Bodie, N. Robinson, G. Armstrong, M. Ward, M. Przetak, G. L. Carter, and R. LaCost.** 1991. Commercial levels of chymosin production by *Aspergillus*. Bio/Technology 9:976–981.
10. **Frischmeyer, P. A., A. van Hoof, K. O'Donnell, A. L. Guerrerio, R. Parker, and H. C. Dietz.** 2002. An mRNA surveillance mechanism that eliminates transcripts lacking termination codons. Science 295:2258–2261.
11. **Galagan, J. E., S. E. Calvo C. Cuomo, L.-J. Ma, J. Wortman, S. Batzoglou,**

S.-I. Lee, M. Baştürkmen, C. C. Spevak, J. Clatterbuck, V. Kapitonov, J. Jurka, C. Scazzocchio, M. Farman, J. Butler, S. Purcell, S. Harris, G. H. Braus, O. Draht, S. Busch, C. D'Enfert, C. Bouchier, G. H. Goldman, D. Bell-Pedersen, S. Griffiths-Jones, J. H. Doonan, J. Yu, K. Vienken, A. Pain, M. Freitag, E. U. Selker, D. B. Archer, M. Á. Peñalva, B. R. Oakley, M. Momany, T. Tanaka, T. Kumagai, K. Asai, M. Machida, W. C. Nierman, D. W. Denning, M. Caddick, M. Hynes, M. Paoletti, R. Fischer, B. Miller, P. Dyer, M. S. Sachs, S. A. Osmani, and B. Birren. 2005. Sequencing of *Aspergillus nidulans* and comparative analysis with *A. fumigatus* and *A. oryzae*. Nature 438:1105–1115.

12. **Gomi, K., Y. Iimura, and S. Hara.** 1987. Integrative transformation of *Aspergillus oryzae* with a plasmid containing the *Aspergillus nidulans argB* gene. Agric. Biol. Chem. 51:2549–2555.
13. **Gooch, V. D., A. Mehra, L. F. Larrondo, J. Fox, M. Touretoutoundis, J. J. Loros, and J. C. Dunlap.** 2008. Fully codon-optimized luciferase uncovers novel temperature characteristics of the *Neurospora* clock. Eukaryot. Cell 7:28–37.
14. **Gouka, R. J., P. J. Punt, J. G. M. Hessing, and C. A. M. J. J. van den Hondel.** 1996. Analysis of heterologous protein production in defined recombinant *Aspergillus awamori* strains. Appl. Environ. Microbiol. 62:1951–1957.
15. **Gouka, R. J., P. J. Punt, and C. A. M. J. J. van den Hondel.** 1997. Glucoamylase gene fusions alleviate limitations for protein production in *Aspergillus awamori* at the transcriptional and (post)translational levels. Appl. Environ. Microbiol. 63:488–497.
16. **Gouka, R. J., P. J. Punt, and C. A. M. J. J. van den Hondel.** 1997. Efficient production of secreted proteins by *Aspergillus*: progress, limitations and prospects. Appl. Microbiol. Biotechnol. 47:1–11.
17. **Graber, J. H., C. R. Cantor, S. C. Mohr, and T. F. Smith.** 1999. *In silico* detection of control signals: mRNA 3′-end-processing sequences in diverse species. Proc. Natl. Acad. Sci. USA 96:14055–14060.
18. **Graber, J. H., G. D. McAllister, and T. F. Smith.** 2002. Probabilistic prediction of *Saccharomyces cerevisiae* mRNA 3′-processing sites. Nucleic Acids Res. 30:1851–1858.
19. **Gustafsson, C., S. Govindrajan, and J. Minshull.** 2004. Codon bias and heterologous protein expression. Trends Biotechnol. 22:346–353.
20. **Hu, J., C. S. Lutz, J. Wilusz, and B. Tian.** 2005. Bioinformatic identification of candidate *cis*-regulatory elements involved in human mRNA polyadenylation. RNA 11:1485–1493.
21. **Hu, S., L. Li, J. Qiao, Y. Guo, L. Cheng, and J. Liu.** 2006. Codon optimization, expression, and characterization of an internalizing anti-ErbB2 single-chain antibody in *Pichia pastoris*. Protein Expr. Purif. 47:249–257.
22. **Ikemura, T.** 1981. Correlation between the abundance of *Escherichia coli* transfer RNAs and the occurrence of the respective codons in its protein genes: a proposal for a synonymous codon choice that is optimal for the *E. coli* translational system. J. Mol. Biol. 151:389–409.
23. **Jacquet, A., M. Magi, H. Petry, and A. Bollen.** 2002. High-level expression of recombinant house dust mite allergen Der p 1 in *Pichia pastoris*. Clin. Exp. Allergy 32:1048–1053.
24. **Kane, J. F.** 1995. Effects of rare codon clusters on high-level expression of heterologous proteins in *Escherichia coli*. Curr. Opin. Biotechnol. 6:494–500.
25. **Kane, J. F., B. N. Violand, D. F. Curan, N. R. State, K. L. Duffin, and G. Bogosian.** 1992. Novel in-frame two codon translational hop during synthesis of bovine placental lactogen in a recombinant strain of *Escherichia coli*. Nucleic Acids Res. 20:6707–6712.
26. **Kawamoto, S., T. Aki, M. Yamashita, A. Tategaki, T. Fujimura, S. Tsuboi, T. Katsutani, O. Suzuki, S. Shigeta, Y. Murooka, and K. Ono.** 2002. Toward elucidating the full spectrum of mite allergens—state of the art. J. Biosci. Bioeng. 94:285–298.
27. **Koda, A., T. Bogaki, T. Minetoki, and M. Hirotsune.** 2005. High expression of a synthetic gene encoding potato alpha-glucan phosphorylase in *Aspergillus niger*. J. Biosci. Bioeng. 100:531–537.
28. **Kofman, A., M. Graf, L. Deml, H. Wolf, and R. Wagner.** 2003. Codon usage-mediated inhibition of HIV-1 gag expression in mammalian cells occurs independently of translation. Tsitologiia 45:94–100.
29. **Kozak, M.** 2005. Regulation of translation via mRNA structure in prokaryotes and eukaryotes. Gene 361:13–37.
30. **Laemmli, U. K.** 1970. Cleavaged structural proteins during assembly of the head of bacteriophage T4. Nature 227:680–685.
31. **Loke, J. C., E. A. Stahlberg, D. G. Strenski, B. J. Haas, P. C. Wood, and Q. Q. Li.** 2005. Compilation of mRNA polyadenylation signals in *Arabidopsis* revealed a new signal element and potential secondary structures. Plant Physiol. 138:1457–1468.
32. **Machida, M., K. Asai, M. Sano, T. Tanaka, T. Kumagai, G. Terai, K. Kusumoto, T. Arima, O. Akita, Y. Kashiwagi, K. Abe, K. Gomi, H. Horiuchi, K. Kitamoto, T. Kobayashi, M. Takeuchi, D. W. Denning, J. E. Galagan, W. C. Nierman, J. Yu, D. B. Archer, J. W. Bennett, D. Bhatnagar, T. E. Cleveland, N. D. Fedorova, O. Gotoh, H. Horikawa, A. Hosoyama, M. Ichinomiya, R. Igarashi, K. Iwashita, P. R. Juvvadi, M. Kato, Y. Kato, T. Kin, A. Kokubun, H. Maeda, N. Maeyama, J. Maruyama, H. Nagasaki, T. Nakajima, K. Oda, K. Okada, I. Paulsen, K. Sakamoto, T. Sawano, M. Takahashi, K. Takase, Y. Terabayashi, J. R. Wortman, O. Yamada, Y. Yamagata, H. Anazawa, Y. Hata, Y. Koide, T. Komori, Y. Koyama, T. Minetoki, S. Suharnan, A. Tanaka, K. Isono, S. Kuhara, N. Ogasawara, and H. Kikuchi.** 2005. Genome sequencing and analysis of *Aspergillus oryzae*. Nature 438:1157–1161.
33. **Maeda, H., M. Sano, Y. Maruyama, T. Tanno, T. Akao, Y. Totsuka, M. Endo, R. Sakuradа, Y. Yamagata, M. Machida, O. Akita, F. Hasegawa, K. Abe, K. Gomi, T. Nakajima, and Y. Iguchi.** 2004. Transcriptional analysis of genes for energy catabolism and hydrolytic enzymes in the filamentous fungus *Aspergillus oryzae* using cDNA microarrays and expressed sequence tags. Appl. Microbiol. Biotechnol. 65:74–83.
34. **Mizutani, O., A. Nojima, M. Yamamoto, K. Furukawa, T. Fujioka, Y. Yamagata, K. Abe, and T. Nakajima.** 2004. Disordered cell integrity signaling caused by disruption of the *kexB* gene in *Aspergillus oryzae*. Eukaryot. Cell 3:1036–1048.
35. **Nelson, G., O. Kozlova-Zwinderman, A. J. Collis, M. R. Knight, J. R. S. Fincham, C. P. Stanger, A. Renwick, J. G. M. Hessing, P. J. Punt, C. A. M. J. J. van den Hondel, and N. D. Read.** 2004. Calcium measurement in living filamentous fungi expressing codon-optimized aequorin. Mol. Microbiol. 52:1437–1450.
36. **Nierman, W. C., A. Pain, M. J. Anderson, J. R. Wortman, H. S. Kim, J. Arroyo, M. Berriman, K. Abe, D. B. Archer, C. Bermejo, J. Bennett, P. Bowyer, D. Chen, M. Collins, R. Coulsen, R. Davies, P. S. Dyer, M. Farman, N. Fedorova, N. Fedorova, T. V. Feldblyum, R. Fischer, N. Fosker, A. Fraser, J. L. Garcia, M. J. Garcia, A. Goble, G. H. Goldman, K. Gomi, S. Griffith-Jones, R. Gwilliam, B. Haas, H. Haas, D. Harris, H. Horiuchi, J. Huang, S. Humphray, J. Jimenez, N. Keller, H. Khouri, K. Kitamoto, T. Kobayashi, S. Konzack, R. Kulkarni, T. Kumagai, A. Lafon, J. P. Latge, W. Li, A. Lord, C. Lu, W. H. Majoros, G. S. May, B. L. Miller, Y. Mohamoud, M. Molina, M. Monod, I. Mouyna, S. Mulligan, L. Murphy, S. O'Neil, I. Paulsen, M. A. Penalva, M. Pertea, C. Price, B. L. Pritchard, M. A. Quail, E. Rabbinowitsch, N. Rawlins, M. A. Rajandream, U. Reichard, H. Renauld, G. D. Robson, S. Rodriguez de Cordoba, J. M. Rodriguez-Pena, C. M. Ronning, S. Rutter, S. L. Salzberg, M. Sanchez, J. C. Sanchez-Ferrero, D. Saunders, K. Seeger, R. Squares, S. Squares, M. Takeuchi, F. Tekaia, G. Turner, C. R. Vazquez de Aldana, J. Weidman, O. White, J. Woodward, J. H. Yu, C. Fraser, J. E. Galagan, K. Asai, M. Machida, N. Hall, B. Barrell, and D. W. Denning.** 2005. Genomic sequence of the pathogenic and allergenic filamentous fungus *Aspergillus fumigatus*. Nature 438:1151–1156.
37. **Outchkourov, S. N., W. J. Stickema, and M. A. Jongsma.** 2002. Optimization of the expression of equistatin in *Pichia pastoris*. Protein Expr. Purif. 24:18–24.
38. **Prodromou, C., and L. H. Pearl.** 1992. Recursive PCR: a novel technique for total gene synthesis. Protein Eng. 5:827–829.
39. **Punt, P. J., N. van Biezen, A. Conesa, A. Alvers, J. Mangnus, and C. A. M. J. J. van den Hondel.** 2002. Filamentous fungi as cell factories for heterologous protein production. Trends Biotechnol. 20:200–2006.
40. **Sambrook, J., E. F. Fritsh, and T. Maniatis.** 1989. Molecular cloning: a laboratory manual, 2nd ed. Cold Spring Harbor Laboratory Press, Cold Spring Harbor, NY.
41. **Scholtmeijer, K., H. A. B. Wösten, J. Springer, and J. G. T. Wessels.** 2001. Effect of introns and AT-rich sequences on expression of the bacterial hygromycin B resistance gene in the basidiomycete *Schizophyllum commune*. Appl. Environ. Microbiol. 67:481–483.
42. **Schuren, F. H. J., and J. G. T. Wessels.** 1998. Expression of heterologous genes in *Schizophyllum commune* is often hampered by the formation of truncated transcripts. Curr. Genet. 3:151–156.
43. **Shen, H. D., K. Y. Chua, W. L. Lin, K. H. Hsieh, and W. R. Thomas.** 1995. Molecular cloning and immunological characterization of the house dust mite allergen Der f 7. Clin. Exp. Allergy 25:1000–1006.
44. **Sheji, H., H. Horiuchi, and M. Takagi.** 1999. Production of recombinant Der fl (a major mite allergen) by *Aspergillus oryzae*. Biosci. Biotechnol. Biochem. 63:703–709.
45. **Sinclair, G., and F. Y. Choy.** 2002. Synonymous codon usage bias and the expression of human glucocerebrosidase in the methylotrophic yeast, *Pichia pastoris*. Protein Expr. Purif. 26:96–105.
46. **Tamalampudi, S., M. M. T. Rahman, S. Hama, Y. Suzuki, A. Kondo, and H. Fukuda.** 2007. Development of recombinant *Aspergillus oryzae* whole-cell biocatalyst expressing lipase-encoding gene from *Candida antarctica*. Appl. Microbiol. Biotechnol. 75:387–395.
47. **Te'o, V. S. J., A. E. Cziferszky, P. L. Bergquist, and K. M. H. Nevallainen.** 2000. Codon optimization of xylanase gene *xynB* from the thermophilic bacterium *Dictoglomus thermophilum* for expression in the filamentous fungus *Trichoderma reesei*. FEMS Microbiol. Lett. 190:13–19.
48. **van Hoof, A., P. A. Frischmeyer, H. C. Dietz, and R. Parker.** 2002. Exosome-mediated recognition and degradation of mRNAs lacking a termination codon. Science 295:2262–2264.
49. **Ward, P. P., C. S. Piddington, G. A. Cunningham, X. Zhou, R. D. Wyatt, and O. M. Conneely.** 1995. A system for production of commercial quantities of human lactoferrin: a broad spectrum natural antibiotic. Bio/Technology 13:498–503.
50. **Wu, X., H. Jornvall, D. B. Kurt, and U. Opperman.** 2004. Codon optimization reveals critical factors for high level expression of two rare codon genes in *Escherichia coli*: RNA stability and secondary structure but not tRNA abundance. Biochem. Biophys. Res. Commun. 313:89–96.

51. **Xia, X.** 1998. How optimized is the translational machinery in *Escherichia coli*, *Salmonella typhimurium* and *Saccharomyces cerevisiae*? Genetics **149:** 37–44.
52. **Yamada, O., B. R. Lee, and K. Gomi.** 1997. Transformation system for *Aspergillus oryzae* with double auxotrophic mutations, *niaD* and *sC*. Biosci. Biotechnol. Biochem. **61:**1367–1369.
53. **Yasuhara, T., T. Takai, T. Yuuki, H. Okudaira, and Y. Okumura.** 2001. Biologically active recombinant forms of a major house dust mite group 1 allergen Der f 1 with full activities of both cysteine protease and IgE binding. Clin. Exp. Allergy **31:**116–124.
54. **Yuuki, T., Y. Okumura, T. Ando, H. Yamakawa, M. Suko, M. Haida, and H. Okudaira.** 1991. Cloning and expression of cDNA coding for the major house dust mite allergen Der f II in *Escherichia coli*. Agric. Biol. Chem. **55:**1233–1238.

Biochemical and Biophysical Research Communications 379 (2009) 681–685

Contents lists available at ScienceDirect

Biochemical and Biophysical Research Communications

journal homepage: www.elsevier.com/locate/ybbrc

SLPI prevents cytokine release in mite protease-exposed conjunctival epithelial cells

Takahiko Seto [a,b], Toshiro Takai [a,*], Nobuyuki Ebihara [b], Hiroyuki Matsuoka [c], Xiao-Ling Wang [a], Akira Ishii [c], Hideoki Ogawa [a], Akira Murakami [b], Ko Okumura [a]

[a] Atopy (Allergy) Research Center, Juntendo University School of Medicine, 2-1-1 Hongo, Bunkyo-ku, Tokyo 113 8421, Japan
[b] Department of Ophthalmology, Juntendo University School of Medicine, Tokyo, Japan
[c] Division of Medical Zoology, Jichi Medical University, Tochigi, Japan

ARTICLE INFO

Article history:
Received 9 December 2008
Available online 25 December 2008

Keywords:
Ocular conjunctival epithelial cells
House dust mite
Serine protease
Proinflammatory cytokine response
Innate antiproteases
Secretory leukocyte protease inhibitor
α1-antitrypsin
Allergic conjunctivitis

ABSTRACT

House dust mites are a major source of allergens associated with allergic diseases including allergic conjunctivitis. Here, we demonstrate that mite-derived serine protease activity induces the release of cytokines from human ocular conjunctival epithelial cells *in vitro* and innate antiproteases, secretory leukocyte protease inhibitor (SLPI) and α1-antitrypsin, can inhibit the response. An extract prepared from a whole-mite culture induced the release of IL-6 and IL-8 and upregulated their gene expression in the human conjunctival epithelial cell line Chang, responses which were inhibited not only by a synthetic serine protease-specific inhibitor, AEBSF, but also by SLPI and α1-antitrypsin at a physiologically relevant concentration. The findings suggest a homeostatic role for SLPI and α1-antitrypsin against the proteases contained in allergen sources in the ocular conjunctiva and that exposure to house dust particles containing mite-derived serine protease activity could be involved in the initiation of sensitization through the ocular conjunctival epithelium and/or exacerbation of allergic conjunctivitis.

Allergic conjunctivitis is caused by direct exposure of the ocular mucosal surfaces to the environment and is the most common hypersensitivity response of the eye [1]. Even seasonal allergenic conjunctivitis and perennial allergic conjunctivitis, ones of the milder and the most common forms of allergic conjunctivitis, have symptoms of itching, tears, mucosal discharge, and redness and a significant clinical and socioeconomic impact because it markedly affects quality of life. One of the major sources of allergens in perennial allergic conjunctivitis is house dust mites of two species, *Dermatophagoides farinae* and *Dermatophagoides pteronyssinus*. Approximately 40% of patients with perennial allergic conjunctivitis have IgE antibodies specific to mite allergens.

Recently, molecules produced by allergen-producing organisms have been suggested to be involved in the pathogenesis of allergic diseases through sensitization and/or exacerbation via IgE-independent mechanisms [2–8]. Airway and ocular conjunctival epithelia and skin epidermis are located at the interface between the body and environment and have critical roles in the response to various stimuli during the sensitization and effecter phases in allergic diseases [2,9]. Ragweed pollen-derived NADPH oxidase has critical roles in both the sensitization and development of asthma [7] and allergic conjunctivitis [8] in mouse models. House dust mites produce serine and cysteine proteases, which have various biological activities including reduction of the functions of tissue barriers and stimulate airway epithelial cells to release proinflammatory cytokines [2–4,10–13].

The mite-derived serine protease activity stimulates airway epithelial cells [12,13], however, its actions on ocular conjunctival epithelial cells have not been investigated. Here, we examine the release of IL-6 and IL-8 from human conjunctival epithelial cells stimulated *in vitro* with a whole-mite culture extract of *D. farinae* containing significant serine protease activity and its inhibition by major innate antiproteases at the ocular mucosa, secretory leukocyte protease inhibitor (SLPI) and α1-antitrypsin [14].

Materials and Methods

Whole mite culture extract. Whole-mite culture extract (WCE) was prepared from a whole culture of *D. farinae* as previously described [15]. Briefly, mites were cultured for one month. PBS was added to the whole culture and gently rotated for 30 min. After centrifugation, the supernatant was filtered for sterilization, and stored at −80 °C prior to use. The protein concentration was deter-

Abbreviations: AEBSF, 4-(2-aminoethyl) benzenesulfonyl fluoride hydrochloride; PAR, protease-activated receptor; SLPI, secretory leukocyte protease inhibitor; WCE, whole mite culture extract of *Dermatophagoides farinae*.

* Corresponding author. Fax: +81 3 3813 5512.
E-mail address: t-takai@juntendo.ac.jp (T. Takai).

0006-291X/$ - see front matter © 2008 Elsevier Inc. All rights reserved.
doi:10.1016/j.bbrc.2008.12.060

mined by the Bradford procedure with a protein assay kit using bovine IgG as the standard (Bio-rad, Richmond, CA).

Culture of ocular conjunctival epithelial cells. Human conjunctival epithelial cells, the Wong Kilborne derivative of Chang epithelial cells, were obtained from American Tissue Type Culture Collection. The conjunctival epithelial cells were cultured in 199 Hanks' medium (Gibco BRL, Carlsbad, CA) supplemented with 10% FCS.

Cells were detached by incubating a monolayer of the cells with a pre-warmed trypsin-EDTA solution for 5 min at 37 °C. Trypsin-neutralizing solution (Cambrex, Walkersville, MD) was added to the cell suspension, and cells were formed into pellets by centrifugation at 210 g for 5 min. The cells were resuspended in culture medium, counted by trypan blue exclusion to determine the viable cell number, and plated at 1.2×10^4 cells/well in 96-well plates, 2.5×10^4 cells/well in 48-well plates, or 1.0×10^5 cells/well in 12-well plates (Corning, Corning, NY). The cultures were incubated in a humidified atmosphere containing 5% CO_2 at 37 °C.

Stimulation of ocular conjunctival epithelial cells. The cells grown to 80% confluence were cultured in FCS-negative medium for 6–12 h, washed, and then stimulated with the WCE (5 or 10 μg/ml). In some experiments, the WCE was pretreated with 0.5 mM E-64 (Peptide Institute, Osaka, Japan) and/or 7.5 mM 4-(2-aminoethyl) benzenesulfonyl fluoride hydrochloride (AEBSF; Sigma, St. Louis, MO) for 30 min at 37 °C and diluted, or recombinant human SLPI (R&D systems, Minneapolis, MN) or purified human α1-antitrypsin (Sigma) was added to the medium at a final concentration of 100 nM. Final concentrations of E-64 and AEBSF were 3.9 μM and 58 μM, respectively.

ELISA. Concentrations of IL-6 and IL-8 in the culture supernatant of cells were measured with ELISA kits (DuoSet; R&D Systems).

Real-time quantitative PCR. Total RNA was extracted from cells using RNAspin Mini (GE Healthcare, Buckinghamshire, UK) and treated with DNase I (GE Healthcare) or an RNeasy Plus Micro Kit (QIAGEN, Hilden, Germany). cDNA was synthesized with SuperScriptII reverse transcriptase (Invitrogen, Carlsbad, CA) and random primers. Real-time quantitative PCR was performed with a TaqMan method using ABI 7500 (Applied Biosystems, Piscataway, NJ). The mRNA level was normalized to the gene expression of glyceraldehyde-3-phosphate dehydrogenase or β-actin.

Statistics. The significance of differences in mean responses was determined with one-way ANOVA and Tukey's *post hoc* test or Student's *t*-test (two-tailed). A value of $p < 0.05$ was regarded as statistically significant. Data shown are representative of three independent experiments.

Results

Whole-mite culture extract induced the release of IL-8 and IL-6 from human ocular conjunctival epithelial cells

We examined whether WCE stimulates ocular conjunctival epithelial cells to release IL-8 and IL-6 (Fig. 1). Because WCE is a soluble extract prepared by the mild agitation of a whole-mite culture containing mite fecal pellets, body fragments, and also residual feed for the mites' growth, we used fresh feed for mites without the addition of live mites as a negative control. The 24-h stimulation with WCE upregulated the release of IL-8 and IL-6, whereas the feed alone did not (Fig. 1A and C). Concentrations of IL-8 and IL-6 in the culture supernatant increased rapidly until 6 h after the stimulation and slowly after that (Fig. 1B and D).

Whole-mite culture extract-induced release of IL-8 and IL-6 was dependent on the serine protease activity

As the WCE exhibited major serine protease activity and minor cysteine protease activity in analyses using fluorogenic synthetic peptide substrates and irreversible class-specific inhibitors (data

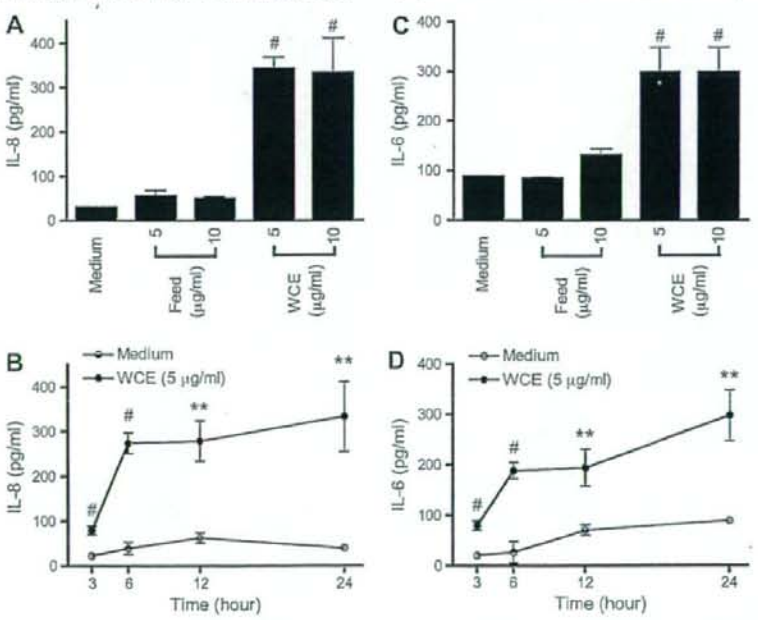

Fig. 1. Whole-mite culture extract induced the release of IL-8 and IL-6 from the human ocular conjunctival epithelial cells. The human ocular conjunctival epithelial cell line Chang was stimulated with whole-mite culture extract (*WCE*), the feed for mites before the addition of live mites as a negative control (*Feed*) at the protein concentrations indicated, or basal medium alone (*Medium*) in 96-well plates (150 μl/well). The culture supernatant was collected at 24 h (**A** and **C**) or at 3, 6, 12, and 24 h (**B** and **D**) and subjected to ELISA. The data indicated are the mean ± SD for three wells and representative of three independent experiments with similar results. $^{*}p < 0.05$, $^{**}p < 0.01$ and $^{\#}p < 0.001$ by one-way ANOVA and Tukey's *post hoc* test compared with *Medium* (**A** and **C**) and *t*-test compared with *Medium* (**B** and **D**).